Physics – Uspekhi **66** (4) 360 – 380 (2023)

REVIEWS OF TOPICAL PROBLEMS PACS numbers: 42.65.Ky, 42.65.Re, **52.38. – r**

Attosecond electromagnetic pulses: generation, measurement, and application. Attosecond metrology and spectroscopy

M Yu Ryabikin, M Yu Emelin, V V Strelkov

DOI: https://doi.org/10.3367/UFNe.2021.10.039078

Contents

Abstract. When intense laser radiation interacts with matter, high-order harmonic generation (HHG) takes place; recent achievements in this area were reported by the authors in a review [V V Strelkov et al. *Phys. Usp.* 59 425 (2016)]. Under certain conditions, the phases of the harmonics can be synchronized in such a way that, adding up, the fields of the harmonics form attosecond ultraviolet (or X-ray) pulses. In this review, we address the generation of a train of attosecond pulses and a single attosecond pulse from a group of high-order harmonics. The problem of measuring the duration of attosecond pulses required both a serious modernization of the measurement methods known in femtosecond optics and the development of fundamentally new approaches. This review describes the main methods for measuring attosecond pulses that have been successfully demonstrated to date. Finally, the use of such pulses to probe the dynamics of electronic processes in matter and to control such processes at attosecond times is discussed.

Keywords: attosecond ultraviolet and X-ray pulses, high-order harmonic generation, interaction of intense laser radiation with matter, phase matching, attosecond metrology, time-resolved nonlinear spectroscopy

Dedicated to the memory of our teacher and co-author Viktor Trifonovich Platonenko (1938–2017)

1. Introduction

In review [1], we considered the phenomenon of high-order harmonic generation (HHG) in an intense laser field, which underlies the methods implemented to date to produce attosecond ultraviolet and X-ray pulses using compact laser systems. The area of application of such pulses can be outlined according to the following considerations. The characteristic oscillation times of atoms in molecules range from tens of picoseconds (for heavy molecules) to about 15 fs (for molecules containing the lightest nuclei — protons). That is why femtosecond lasers have become a tool that has found wide application for studying processes in matter associated with the motion of nuclei. Since an electron is about 2000 times lighter than a proton, the characteristic time scales of the processes caused by the motion of electrons are several orders of magnitude shorter than the corresponding times for the nuclear subsystem. It should be recalled that the Keplerian period for an electron in a hydrogen atom in the first Bohr orbit is about 152 as. Therefore, to probe the electron dynamics, the use of electromagnetic pulses of

M Yu Ryabikin [1,2,a], **M Yu Emelin** [1,b], **V V Strelkov** [3,4,c]
[1] Gaponov-Grekhov Institute of Applied Physics, Russian Academy of Sciences, ul. Ulyanova 46, 603950 Nizhny Novgorod, Russian Federation
[2] Lobachevsky State University of Nizhny Novgorod (National Research University), prosp. Gagarina 23, 603950 Nizhny Novgorod, Russian Federation
[3] Prokhorov General Physics Institute, Russian Academy of Sciences, ul. Vavilova 38, 119991 Moscow, Russian Federation
[4] Moscow Institute of Physics and Technology (National Research University), Institutskii per. 9, 141701 Dolgoprudny, Moscow Region, Russian Federation
E-mail: [a]mikhail.ryabikin@ipfran.ru, [b]emelin@ipfran.ru, [c]strelkov.v@gmail.com

Received 30 July 2021
Uspekhi Fizicheskikh Nauk **193** (4) 382 – 405 (2023)
Translated by M Yu Ryabikin

attosecond duration is required. The production and use of such pulses is the main subject of attosecond physics.

This review is essentially the second part of review [1]. Below, we discuss modern achievements in obtaining pulse trains and single attosecond pulses (APs) and methods for measuring the duration of APs; special attention is paid to the results of key experiments on the use of APs and a discussion of the prospects for further research in this area.

2. Methods for producing attosecond pulses

As is known, the width of a spectrum and the duration of a Fourier limited light pulse are related to each other according to the uncertainty relation between the energy and time for photons: $\Delta E \Delta t \sim \hbar$, where $\hbar$ is Planck's constant. For example, the full width at half maximum (FWHM) of a Fourier limited Gaussian pulse (τ_p) is related to its spectral width ($\Delta\omega$) according to $\tau_p[\text{as}] \approx 1825/(\hbar\Delta\omega\,[\text{eV}])$ [2]. Hence, it is obvious that the width of the spectral interval covered by visible and infrared light is insufficient to obtain pulses with a duration shorter than 0.6 fs; therefore, to obtain attosecond pulses, coherent radiation in the ultraviolet or X-ray range is necessary. It should also be noted that, for the main practical applications of attosecond radiation, the repeatability of its characteristics from pulse to pulse and the possibility of its high-precision synchronization with an external signal (usually in the optical range) are important. The only approach that has been developed to date that ensures the reliable fulfillment of all these requirements is the generation of high-order harmonics of optical radiation. As shown in [1], the coherence of the HHG process leads to the fact that the phases of high-order harmonics are related to the phase of the generating radiation, and thus to each other (note that such a relationship can often be very complex due to the quantum interference of various contributions to nonlinear polarization at the frequency of one harmonic or another (see Fig. 4 in [1])). This fundamental feature is determined by the microscopic generation mechanism; it is also preserved in the macroscopic response of the generating medium. The phasing of the harmonics determines the possibility of obtaining APs from them, as noted in the first studies [3–5], which proposed such a method for producing short electromagnetic pulses. The main results on AP production have been achieved using the generation of harmonics in gases, and therefore we will consider this particular case below (the calculations for producing APs using generation in plasma are presented in [1, Section 3] (see also [6, 7])).

2.1 Generation of a train of attosecond pulses. Selection of electron trajectories

An analysis of the HHG process within the framework of the semiclassical three-step model [8] or its quantum mechanical analog [9] shows that the key role in the emission of high-frequency radiation by atoms ionized by an intense laser pulse is played by two types of trajectories of electrons released from the atom and after some time τ returning to the parent ion. Trajectories corresponding to the electron release at phases $108^\circ < \varphi < 180^\circ$ of a sinusoidal field and, accordingly, the time $0 < \tau < 0.65T$ of its free motion (T is the period of the fundamental field) are called *short* trajectories; the rest are *long*. The release of an electron at a field phase equal to 108° leads to its maximum energy gain by the time it returns to the parent ion; it is this energy that determines the harmonic order corresponding to the high-frequency cutoff in the HHG spectrum: $N_{\max} \approx (I_p + 3.17U_p)/(\hbar\omega_0)$, where I_p is the ionization potential of an atom, $U_p = e^2E_0^2/(4m\omega_0^2)$ is the oscillatory ('ponderomotive') energy of an electron, and E_0 and ω_0 are the amplitude and frequency of the laser field. Note that the quadratic dependence of the ponderomotive energy on the laser wavelength $\lambda_0 = 2\pi c/\omega_0$ determines the advantages of using long-wavelength laser sources to obtain broadband harmonic radiation (for details, see [1]).

Analyses show (see the consideration given in [1, Section 2.2] and the literature cited therein) that, in order to obtain APs from the group of high-order harmonics (HH), it is necessary to select the contribution of electron trajectories of only one type. The pulse generated by this contribution has a certain sign of the chirp (called an *attochirp*), namely, for the short trajectory contribution, the radiation frequency increases with time, while for the long trajectory contribution, it decreases. Then, a Fourier limited pulse can be obtained by compensating the attochirp of the selected radiation component by passing it through a dispersive medium with the appropriate sign and value of dispersion in the frequency range of interest.

One of the methods for selecting the contributions of particular electron trajectories to the harmonic signal is based on the special choice of the geometry of the experiment. As was noted in [1], for different path contributions, the dependence of the phase on the laser intensity is different (both contributions increase approximately in proportion to the intensity, but for long trajectories, the proportionality factor is, as a rule, much larger than for short ones [10–12]). This leads to the fact that, for different contributions, the phase-matching conditions turn out to be satisfied at slightly different positions of the generating medium relative to the focus of the laser beam. In particular, when the laser beam is focused at a certain point in front of the gas jet, the phase-matching conditions can be satisfied for a short trajectory and not for the rest, which leads to selection of the contribution of this trajectory [4, 13, 14]. This method was used in the first experiments on producing AP trains [15], where the radiation of five neighboring harmonics was summed. Further experiments showed the possibility of obtaining AP trains from a wider spectral range [16, 17] (see also reviews [18, 19]).

Another way to select the contributions of different electron trajectories is related to the different divergence of harmonic beams generated due to different contributions. The wavefront of harmonic radiation differs from the wavefront of the generating field [20–22] due to the dependence of the harmonic phase on the intensity of the generating radiation, which varies along the beam radius. The difference in this dependence for different contributions leads to various divergences of the harmonic beams generated due to these contributions. The selection of the contributions of a certain trajectory can be achieved by passing the harmonic beam through a diaphragm [5, 23–25]. This method was used to obtain a train of attosecond pulses in experiment [26].

To compensate for the positive AP chirp [16, 26, 27], filters with the appropriate group velocity dispersion can be used. In experiments [26], the spectral filtering of radiation from ten (from the 17th to the 35th) neighboring odd harmonics in a frequency window about 30 eV wide and their synchronization were carried out using thin aluminum films. In experiments [26], a train of almost Fourier limited APs with a duration of 170 as each was obtained (see below for methods for measuring the duration of attosecond pulses), which amounted to a value close to the limit of about 1.2 field

cycles at the central frequency of the selected radiation (photon energy of about 30 eV). In a series of experiments [28] using other metal or semiconductor filters, pulses were obtained with a spectral width of up to 45 eV and with a central frequency depending on the filter material; the use of zirconium films made it possible to obtain pulses with a duration of 130 as and a central photon energy of about 80 eV.

In view of the importance of the problem of attochirp compensation, the search for ways to solve it is constantly ongoing. Thus, besides thin solid-state filters, the use of other dispersive elements, such as multilayer chirped X-ray mirrors [29–31] and gaseous media [32, 33], have been demonstrated. However, in general, this approach has limitations related to the properties of the materials, such as absorption or the finite width of the spectral range in which the dispersion behaves in the desired manner. Other proposed schemes are based on the use of multicolor and/or chirped laser pulses to control the trajectories of free electrons [34, 35]. Although these schemes can have great flexibility, their implementation in macroscopic volumes of nonlinear media is hampered by such undesirable consequences of dispersion as phase mismatch and deviation of the waveforms of interacting fields from optimal ones during propagation.

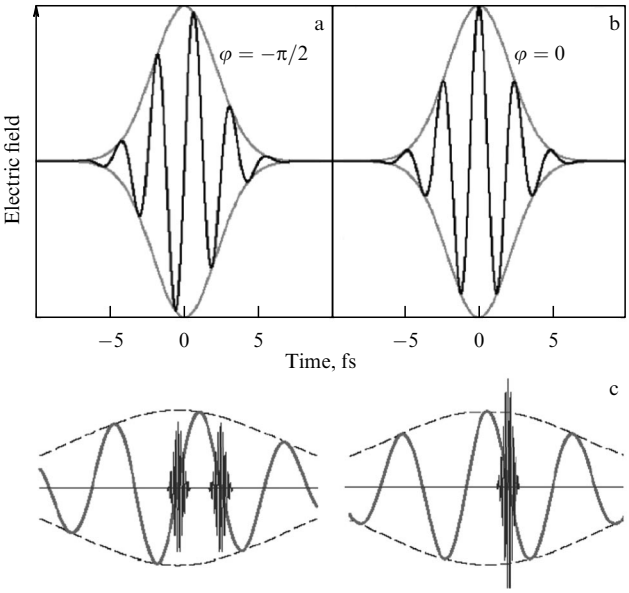

Figure 1. Time profile of the electric field of an ultrashort laser pulse with absolute phase (a) $\varphi = -\pi/2$ and (b) $\varphi = 0$. (c) Time profiles of VUV radiation bursts obtained after selection of the high-frequency part of the spectrum of generated harmonics for the same values of the absolute phase.

2.2 Generation of an isolated attosecond pulse

If ultraviolet or X-ray radiation is generated as a set of phased discrete odd harmonics, then its intensity in time is a train of APs separated by an interval equal to half the generating radiation cycle. To obtain an *isolated* pulse (required for most applications, for example, in pump–probe spectroscopy), some kind of 'shutter' is needed that can open (and close) on such a time scale. The creation of such a high-speed optical element is a difficult task; therefore, the methods for producing an isolated AP developed to date implement gating at the stage of generation of ultraviolet (UV) radiation, rather than when it propagates through an additional optical element. An isolated AP is obtained if generation occurs on only one half-cycle. The generated spectrum is then no longer a set of harmonics, but a continuum. What is important, however, is that the phasing of the spectral components, which is inherent in HHG, is preserved.

The problem of selecting different electron trajectories when producing an isolated AP is similar to that for the case of producing an AP train and is solved by similar methods. The generation time reduction for obtaining a single AP is implemented using various approaches outlined below.

2.2.1 Use of few-cycle laser pulses ('amplitude gating'). Let us consider HHG in the case of a laser pulse containing only several half-cycles of the laser field. For a number of processes in the field of such a pulse, which can be written as $E(t) = E_0(t)\cos(\omega_0 t + \varphi)$, the phase φ of the field relative to the envelope, or the absolute phase of the laser pulse (also referred to as CEP — Carrier-Envelope Phase, or CE phase), plays a significant role [36–46]. In the HHG process, the maximum frequency of UV radiation generated in each laser half-cycle is determined mainly by the instantaneous field amplitude in that half-cycle. Radiation near the cutoff of the plateau is generated only on one half-cycle at the maximum of the laser pulse [47] (at a certain CE phase [48]; see below). Thus, the selection of the highest-frequency part of the generated radiation spectrum makes it possible to obtain an isolated attosecond pulse, which was first experimentally demonstrated in 2001 [29]. The duration of the attopulses obtained in [29] with a photon energy of about 90 eV was 650 as. A fundamental role in the progress of this technique [38] was played by the possibility of stabilizing the CE phase of the generating pulse [49–52].

Figure 1 illustrates the dependence of the time profile of vacuum ultraviolet radiation (VUV radiation) on the absolute phase of a laser pulse with a duration of several field cycles, which is expected from theory and confirmed by spectral measurements in experiment [53]. It can be seen from the figure that, in the case of a sine-like pulse ($\varphi = -\pi/2$), the generated radiation in the region of the plateau cutoff is a pair of attosecond pulses, while for a cosine-like pulse ($\varphi = 0$) it is an isolated pulse. This is explained by the fact that, in the first case ($\varphi = -\pi/2$), the electron return with maximum kinetic energy occurs in two half-cycles of the field, in which the field amplitude is maximum; in the second case ($\varphi = 0$), there is only one such half-cycle, since the electrons returning in the previous and subsequent half-cycles have a significantly lower kinetic energy. In experiment [53], neon atoms were exposed to 5 femtosecond pulses with central wavelength $\lambda = 750$ nm and a controlled CE phase; a two-component multilayer Mo/Si mirror with maximum reflectivity in the region of 93 eV was used as a high-frequency filter. The results of measurements of attosecond pulses confirmed the above picture, while the duration of an isolated VUV radiation pulse in the reflection region of the Mo/Si mirror was 250 as, which was a record-breaking value for that time.

As demonstrated in experiments, the application of this method when using phase-stabilized few-cycle laser pulses and compensation of the attochirp of the generated radiation make it possible to obtain isolated pulses of VUV and soft X-ray radiation with a duration of less than 100 as. For instance, due to the use of a near-IR laser source with a pulse duration of less than 1.5 cycles with a controlled waveform [54] and chirped VUV multilayer mirrors [55], isolated pulses with a duration of about 80 as were obtained in an experiment with neon atoms [30], with an average photon energy of about

80 eV and the brightness as high as about 10^{11} photons per second. In experiment [56], when argon atoms were exposed to radiation from a parametric source with a pulse duration of about two cycles of the field at a central wavelength of 1.8 μm and zirconium foil was used to compensate for the attochirp, pulses with a duration of 43 as and an average photon energy of about 110 eV were obtained. In the absence of dispersive elements, as shown by calculations [12], the minimum duration of APs that can be obtained in argon by this method is 0.08–0.10 of the laser cycle for different intensities and frequencies of the generating field.

2.2.2 Use of laser pulses of varying ellipticity ('polarization gating'). As mentioned in [1], the efficiency of HHG rapidly decreases with increasing laser ellipticity, because, in the elliptically polarized field, an electron 'misses' the parent ion when returning to it; simple expressions for threshold ellipticity (the laser ellipticity at which the HHG efficiency is halved) obtained in [57] are in good agreement with experiment (see, for example, [58]). For what follows, it is important that an ellipticity of 10–15% already leads to a significant decrease in the harmonic generation efficiency. Therefore, in the case of HHG using a laser pulse with a time-varying ellipticity, the generation efficiency will be maximum in the time interval when the polarization is close to linear. If the ellipticity changes sufficiently rapidly (namely, if the duration of this time interval is about half the optical cycle), then the generation of an isolated attosecond pulse is expected [59]. Of course, with such a rapid change in the polarization of the laser field, the very concept of instantaneous ellipticity loses its meaning, so a rigorous study of HHG in this case requires a complete quantum mechanical calculation [60, 61].

Engineering a field with rapidly changing ellipticity is a special problem. In [59], it was proposed that such a field be obtained from two short pulses with different frequencies. A much simpler method was proposed in [62]. The initial laser beam is split into two beams, which are converted into beams of circularly polarized radiation with mutually opposite directions of field rotation and then brought together into one beam with the introduced delay δ between pulses of the order of duration τ of the initial pulse. The polarization of the resulting field is close to circular at the tails of the pulse and is close to linear in its central part. Assuming that HHG occurs as long as the ellipticity is lower than a certain threshold value ε_{th}, one can obtain the following expression for the time interval during which harmonics are generated [63]:

$$\Delta = \frac{\varepsilon_{\text{th}}\tau^2}{\delta \ln 2}\,. \qquad (1)$$

It can be seen that it is possible to shorten the 'time window' Δ by increasing the delay δ or reducing the pulse duration τ. However, for $\delta > \tau$, the intensity of the resulting pump pulse has a dip in the region where the polarization is close to linear, i.e., there is a loss of laser power. Therefore, delays that satisfy the condition $\delta \approx \tau$ are practically used.

In experiments [64], the described method for obtaining a pulse of varying ellipticity was modified. The pump radiation ellipticity was modulated by transmitting the initial beam through two quarter-wave quartz plates (zero-order and high-order), whose axes were oriented in a certain way relative to the direction of polarization of the initial laser pulse (Fig. 2). In this case, the delay δ is determined by the thickness of the high-order quarter-wave plate. Controlling

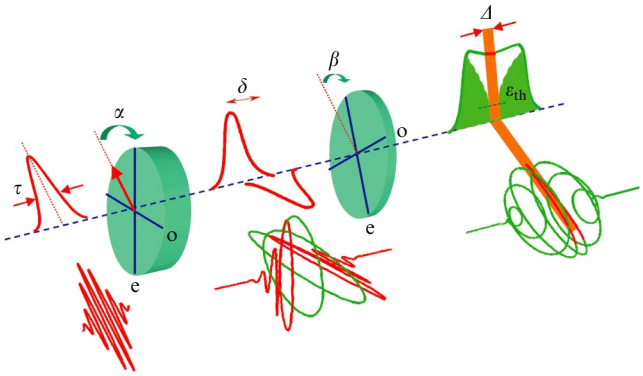

Figure 2. Diagram of a device for obtaining a generating field with a time-varying ellipticity. The orientation of the quarter-wave plates with respect to the polarization of the incoming laser pulse is shown, as is the field after the passage of each plate. After the second plate, the field ellipticity is lower than the threshold ellipticity ε_{th} only at the center of the pulse within the time window of duration Δ shown in the figure.

the angle of rotation of the axis of a zero-order quarter-wave plate makes it possible to *continuously* change the ellipticity profile without changing the intensity profile, i.e., change the duration of the gate time window from the minimum (still set by Eqn (1)) to the maximum, approximately determined by the duration of the generating pulse $(\delta^2 + \tau^2)^{1/2}$. Control of the harmonic pulse duration using this technique was demonstrated in Ref. [65] using laser pulses with a duration of 40 fs.

To obtain an isolated attosecond pulse using this technique, it is necessary that the polarization gate remain open only for a time not exceeding a half-cycle of the laser field. As shown in [66] from a comparison with numerical calculations, Eqn (1), which has a high accuracy for a time window with a duration of several cycles, works satisfactorily in this case as well. Assuming $\varepsilon_{\text{th}} \approx 0.15$, we find from (1) that, to obtain a single attopulse by the polarization gating method, a laser pulse with a duration of several field cycles is required (although longer than in the amplitude gating method); for the wavelength of a Ti:Sapphire laser, the duration of such a pulse is about 6 fs. A very important advantage of the polarization gating method is that it works for all HHs, and not just near the cutoff of the plateau. As in the case of the amplitude gating, an important role in this method is played by the CE phase of the laser pulse, which determines the features of the dynamics of an electron wave packet as it moves in a continuum and, thus, the characteristics of the generated attosecond pulse [61, 63]. Therefore, to obtain attosecond pulses with stable (i.e., not changing from one laser pulse to another) characteristics, a laser pulse with a stabilized absolute phase is required. Such a 5-fs laser pulse was used to obtain a single attosecond pulse in experiment [58] (Figs 3, 4).

The application of this approach in combination with a careful provision of conditions for compensating the attosecond chirp made it possible to obtain isolated pulses with a duration of 130 as [67] and photon energies up to 36 eV when argon atoms were exposed to radiation pulses from a Ti:Sapphire laser with a wavelength of about 750 nm. Moreover, as reported in Ref. [67], the CE phase of attosecond pulses turns out to be stable in this case. The use of a longer-wavelength laser source (with a central wavelength of about 1.8 μm) made it possible, when irradiating neon atoms, to

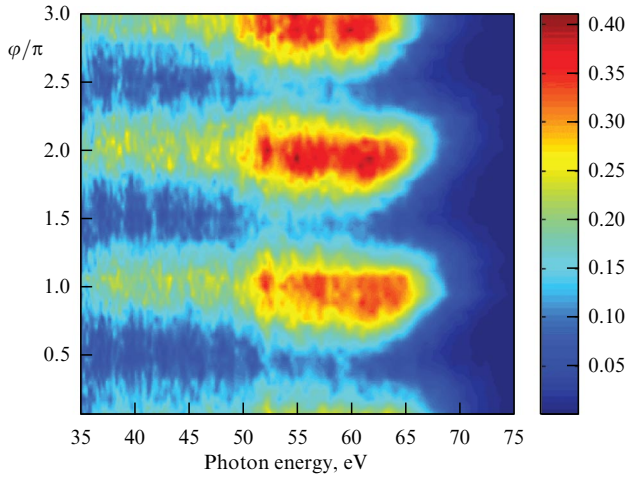

Figure 3. Spectrum of UV radiation measured at various absolute phases of the generating field. (Taken from Ref. [58].)

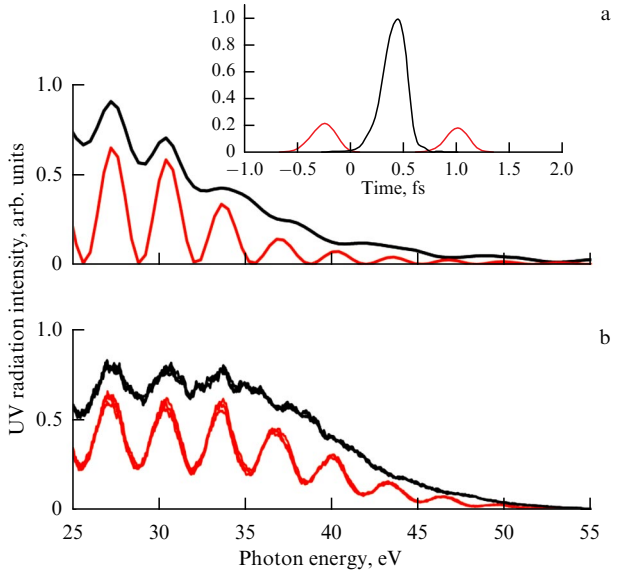

Figure 4. Spectrum of UV radiation for two values of the absolute phase differing by $\pi/2$ calculated theoretically (a) and measured experimentally (b). Inset to Fig. a shows the time dependence of the UV radiation intensity calculated for two values of the absolute phase. (Taken from Ref. [58].)

generate high harmonics with photon energies reaching the K absorption edge of carbon (284 eV); the measured duration of the resulting single harmonic pulse was 53 as [68].

The technique described above was further developed in [69–71], where it was proposed that two elliptically (rather than circularly) polarized pulses be used to obtain a rapidly changing ellipticity. For a certain orientation of the polarization ellipses, expression (1) becomes [71]

$$\Delta = \xi \frac{\varepsilon_{\text{th}} \tau^2}{\delta \ln 2}, \qquad (2)$$

where ξ is the ellipticity of the initial pulses. In this case, there must be $\xi > \varepsilon_{\text{th}}$ in order to suppress HHG at the tails of the resulting pulse [70] (where the ellipticity is close to ξ). As can be seen from a comparison of Eqns (1) and (2), this technique makes it possible to use approximately $1/\xi$ times longer laser pulses to obtain the same window duration Δ. We also note that in [69, 70] a modified scheme ('interferometric polarization gating') was exploited, based on the use of devices such as Michelson [69] or Mach–Zehnder [70] interferometers instead of birefringent elements; such devices are promising for operation with high-intensity laser pulses. In [69], using laser pulses with a duration of 50 fs, a nearly continuous spectrum corresponding to an attosecond pulse with a duration of 340 as was obtained with this method.

2.2.3 Use of fast ionization of a medium ('ionization gating'). The HHG efficiency decreases as the generating atoms are ionized (their ground state is depleted). Thus, if deep ionization of the medium occurs during the time of the laser pulse, then the duration of the harmonic pulse is limited by the time during which ionization takes place. Ionization occurring during a time of the order of the optical cycle duration will make it possible to obtain a single attosecond pulse, as proposed in [72–74]. Such fast ionization requires not only a high peak intensity of the pulse but also a short duration of its leading edge (otherwise, ionization will begin long before the pulse maximum). Therefore, the use of ionization gating requires very short laser pulses (apparently, even shorter than in other methods for producing an isolated attosecond pulse). An important feature of this method is that it limits the generation time of all HHs, rather than just harmonics in the region of the plateau cutoff (as is the case for the amplitude gating method). In a more realistic case (especially for high-intensity laser pulses required for the implementation of ionization gating), the leading edge of the laser pulse contains at least several half-cycles of the field. Then, relatively low-frequency initial bursts of harmonics generated at the leading edge can be blocked using spectral filtering (at the cost of reducing the spectral width and, consequently, increasing the duration of the generated useful pulse); in this case, the method becomes more similar to the amplitude gating method.

2.2.4 Use of time-dependent phase mismatch. The approaches discussed above to produce an isolated attosecond pulse involve the use of generating pulses with a stabilized CE phase. However, the absolute phase of existing laser systems has limited long-term stability, and the energy of such pulses is limited, as a rule, to several hundred microjoules. Due to the low efficiency of high harmonic generation, this leads to the fact that the energy of the resulting attosecond pulses is limited to the nanojoule (or even subnanojoule) range. Such a low energy of attosecond pulses significantly limits the scope of their application. On the other hand, pulses of high harmonics with energies at the level of microjoules are currently experimentally available [75, 76]; record high values reach 100–200 μJ in the photon energy range up to 30 eV [77]. These values of the harmonic emission power, however, are achievable with HHG driven by relatively long laser pulses without stabilization of the CE phase. The use of such laser pulses to generate an *isolated* attosecond pulse will significantly increase its energy and make the sources of attosecond pulses more accessible. Increasing the energy of an attosecond pulse will make it possible to study nonlinear optical phenomena in the attosecond range; in view of this, the problem of increasing the energy of attosecond pulses seems to merit much attention.

High-energy attosecond pulses can be obtained using a technique based on controlling the temporal dynamics of the *macroscopic* high-frequency response of the medium. As

noted in review [1, Section 2.4], the HHG efficiency strongly depends on the fulfillment of the phase-matching conditions and reaches a maximum when the phase velocities of the harmonic and laser fields are almost equal to each other. The magnitude of the phase mismatch in the process of harmonic generation is determined by the geometry of the experiment, the pressure and type of gas, as well as the density of free electrons, which greatly affects the phase velocity of the laser pulse. The last factor makes the HHG phase matching particularly sensitive to the density of free electrons in the target. At the same time, HHG is always accompanied by ionization of the medium; therefore, the electron density varies with time. Thus, the phase mismatch changes during the laser pulse [78, 79]; therefore, the generation efficiency can be maximum within a certain time window, where the phase mismatch is minimal. If the phase mismatch changes significantly over a time of about half the optical cycle, then only one attopulse can be efficiently generated [80–83]. Such a situation can take place during tunneling ionization, when the density of free electrons increases abruptly near the extrema of the instantaneous values of the laser electric field. The height of the jumps, and therefore the corresponding addition to the phase mismatch, are determined by the laser peak intensity and its time profile, the target thickness, the pressure, and the type of gas.

However, the described simple picture is correct only in the one-dimensional case. Usually, the laser intensity varies across the beam cross section; hence, the degree of ionization is also distributed nonuniformly. This dependence of the density of free electrons on the radius leads to the fact that the position in time of the window of efficient generation of ultraviolet radiation also depends on the radius. Thus, the total effective generation time is increased. Moreover, due to the peculiarities of on-axis and off-axis phase matching, the time structure of attosecond pulses in the far field can change over the beam cross section [84, 85].

To overcome this limitation, it was proposed in [80] to use a laser beam with a special intensity profile, namely, a beam in which the intensity in the target region is almost independent of the radius up to a certain distance from the axis and rapidly decreases at larger distances; Ref. [80] also presents a proposed method for engineering such a beam. The 'flat-top' intensity profile ensures simultaneous ionization across the entire central part of the beam. Note that, in similar beams, the optimization of conditions for achieving a high HHG efficiency was previously experimentally demonstrated [86, 87].

To illustrate the role of time-dependent phase matching, Fig. 5 compares the attopulses generated by a 10-fs laser pulse in a target 0.75 mm thick and in a gas layer 1% as thick. The intensity of radiation generated in a thin gaseous layer is multiplied by the square of the thickness ratio (100^2). The properties of radiation generated in a thin target are determined only by the microscopic response, and not by phase matching. Accordingly, a train of attopulses with a duration of approximately 5 fs is observed. On the contrary, for a thick target, the time of UV emission is limited by time-varying phase matching, as a result of which only one pulse from the train is efficiently generated.

It is important that the time dynamics of the phase mismatch in this case is related to the CE phase of the laser field (since tunneling ionization occurs near the field peaks). Therefore, both the position of the synchronism window in time and the moments of emission of attosecond pulses are determined by the absolute phase. As a result, as calculations show [80], the main characteristics of a single attosecond pulse obtained by this method depend only to a small extent on the CE phase of the laser field.

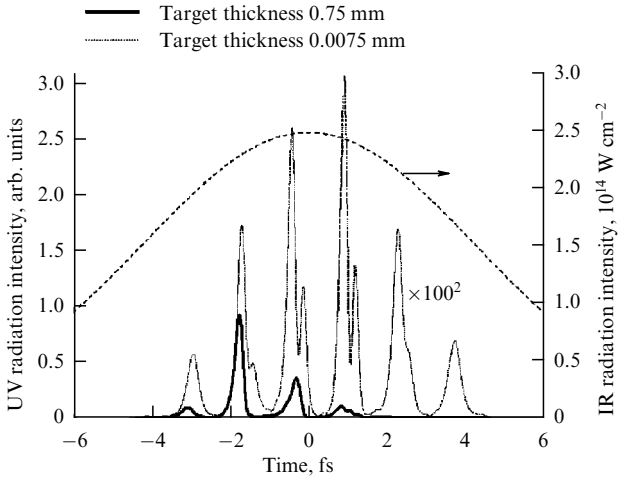

Figure 5. Attosecond pulses generated in argon by a 'flat-top' laser beam in a relatively thick target (0.75 mm) and in a very thin layer. Intensity of UV radiation with frequencies above $32\omega_0$ is shown. As can be seen, a train consisting of several pulses is generated in a thin layer, while in a thick target only one of them is generated efficiently thanks to fulfillment of phase-matching conditions. (Taken from Ref. [80].)

The first experimental results on the generation of harmonics by a flat-top laser beam were published in [88–90].

2.2.5 Use of a two-color field. As was already shown in earlier studies [91, 92], in the case of HHG in an intense laser field and its second harmonic, both odd and even harmonics of the fundamental frequency are present in the harmonic spectrum, and their intensity can be similar even at a relatively low intensity of the second harmonic. This property of the generated spectrum corresponds to an increase in the periodicity of the process from half the optical cycle to the full cycle; in particular, at a certain phase between the fundamental frequency component and the second harmonic, attosecond pulses in a train follow one after another in each cycle (rather than half-cycle) of the laser field [93, 94]. Qualitatively, this property is explained by the fact that the addition of the second harmonic violates the initial symmetry of the pump field: if, at a certain half-cycle of the fundamental frequency, the field of the second harmonic is *added* to the field of the fundamental frequency near the field peak, then at the next half-cycle it is *subtracted* from it. This circumstance leads to different ionization probabilities in these half-cycles and, consequently, to different intensities of the generated attosecond pulses. The very strong dependence of the tunneling ionization probability on the field amplitude leads to the fact that the generation of attosecond pulses can be practically suppressed in every second half-cycle even at a relatively low intensity of the second harmonic. Doubling the repetition period of attosecond pulses in a train obviously doubles the time allowed for the gate to close in order to produce an isolated pulse. Thus, it can be said that the addition of the second harmonic field makes it possible to use pulses that are approximately twice as long in all of the above methods for producing a single attosecond pulse.

In [94], the use of a two-color field for producing an isolated attosecond pulse by the amplitude gating method was proposed. The polarization gating method exploiting generation in a two-color field [95] using a laser source with a pulse duration of 9 fs made it possible to obtain a supercontinuum corresponding to a single pulse with a duration of 130 as. The use of a two-color field and a 'generalized' polarization gate made it possible to obtain in [71] a single attosecond pulse with a duration of 150 as using a laser pulse with a duration of 28 fs. By compensating for the attochirp of a single pulse of harmonics with photon energies from 55 to 130 eV, which was isolated by the polarization gating method from the radiation generated in a two-color field using a laser source with a pulse duration of 7 fs, a harmonic pulse duration of 67 as was achieved, which was record-breakingly short at that time [96]. Calculations in [80] demonstrated the production of a single attosecond pulse in a two-color field due to a variable detuning from phase matching conditions using a laser pulse with a duration of 20 fs. Finally, in [97], it was proposed to use a three-color generating field with incommensurate frequencies to obtain a single attosecond pulse.

Note that the use of a two-color generating field in some cases can significantly enhance the generation efficiency. For example, in a two-color field (fundamental laser field and its orthogonally polarized second harmonic of comparable intensity), a record generation efficiency was obtained [98] (5×10^{-5} for the 38th harmonic of a Ti:Sapphire laser); explanations for the increase in the generation efficiency in a two-color field are proposed in [98–100]. Thus, the use of a two-color field is a promising way to obtain an isolated high-intensity AP.

2.2.6 Use of laser beams with a rotating wavefront ('attosecond lighthouse'). In all the methods for separating a single attosecond pulse from a train of pulses discussed above, an important role is played by the features of the spectral characteristics of the generated radiation and the temporal characteristics of a laser field. Relatively recently, a fundamentally different approach has been proposed, which makes it possible to separate attosecond pulses from the generated sequence along different propagation directions. This method of pulse separation was called the 'attosecond lighthouse' [101]. The method is based on the principle of wavefront rotation [102] in the region where high harmonics are generated (at the focus of the laser beam).

Let the field in the laser pulse before focusing have the following form:

$$E(x_\mathrm{i}, t) = E_0 \exp\left(-2\left[\frac{t-\xi x_\mathrm{i}}{\tau_\mathrm{i}}\right]^2 - 2\,\frac{x_\mathrm{i}^2}{w_\mathrm{i}^2} + \mathrm{i}\omega_\mathrm{L} t\right), \quad (3)$$

where x_i is one of the transverse coordinates, τ_i is the Fourier limited pulse duration, w_i is the beam diameter, ω_L is the central frequency of laser radiation, and ξ is the pulse-front tilt parameter. The pulse given by Eqn (3) is called a pulse with tilted front. It can be obtained by slight misalignment of the grating compressor at the final stage of femtosecond pulse amplification.

The field at the focus $\tilde{E}(k, t)$ is the Fourier transform of the field in front of the lens (given by Eqn (3)), where $k = k_\mathrm{L} x_f/f$, x_f is the transverse coordinate in the focal plane, f is the focal length of the lens, and $k_\mathrm{L} = \omega_\mathrm{L}/c$. It can be shown [103] that, when the pulse (3) is focused, the local frequency of the laser field will depend on x_f:

$$\tilde{E}(x_f, t) \propto \exp\left(-2\,\frac{t^2}{\tau_f^2} - 2\,\frac{x_f^2}{w_f^2}\right) \exp\left[\mathrm{i}\phi(x_f, t)\right],$$

$$\phi(x_f, t) = 4\,\frac{w_\mathrm{i}\xi}{w_f \tau_f \tau_\mathrm{i}}\, x_f t + \omega_\mathrm{L} t, \quad (4)$$

where the pulse duration at the focal point τ_f and the size of the waist w_f along the coordinate x_f are given by

$$\frac{\tau_f}{\tau_\mathrm{i}} = \frac{w_f}{w_0} = \sqrt{1 + \left(\frac{w_\mathrm{i}\xi}{\tau_\mathrm{i}}\right)^2},$$

and $w_0 = 4f/(k_\mathrm{L} w_\mathrm{i})$ is the size of the waist at the focus at $\xi = 0$. The instantaneous direction of light propagation $\beta(t)$ is given by $\beta \approx k_\perp(t)/k_\mathrm{L}$, where $k_\perp(t) = \partial\varphi/\partial x_f$. Since β turns out to be time dependent, the direction of propagation changes with time, namely, the wavefront in the focal plane rotates with the speed given by

$$v_\mathrm{r} = \frac{\mathrm{d}\beta}{\mathrm{d}t} = \frac{w_\mathrm{i}^2}{f\tau_\mathrm{i}^2}\,\frac{\xi}{1 + (w_\mathrm{i}\xi/\tau_\mathrm{i})^2}.$$

The maximum possible value of the speed of rotation of the wavefront for a given pulse duration τ_i and the divergence of optical radiation $\theta_\mathrm{L} = w_\mathrm{i}/f$ is achieved at $\xi = \tau_\mathrm{i}/w_\mathrm{i}$ and is given by $v_\mathrm{r}^{\max} = \theta_\mathrm{L}/(2\tau_\mathrm{i})$.

Since the pulse wavefront in the focal plane rotates when the pulse-front tilt is used, attosecond pulses generated at different times propagate in different directions. To obtain a single pulse in each direction, it is necessary that, during the time between two adjacent generated harmonic bursts, the wavefront rotate by an amount exceeding the divergence of the attosecond pulse, i.e., for a laser pulse with a maximum wavefront rotation speed, we obtain the condition for its maximum duration:

$$N_\mathrm{c} \leqslant \frac{\theta_\mathrm{L}}{\alpha p \theta_n},$$

where N_c is the number of cycles in a laser pulse, p is the number of attosecond pulses generated in each optical period, and α is a coefficient on the order of unity determined by the required contrast between a given attosecond pulse and its nearest neighbors propagating in the same direction.

Since this method is not exclusively tied to the process of high harmonic generation in gases, it can also be applied to other schemes for generating attosecond pulses. The 'attosecond lighthouse' principle was first implemented in an experiment on the generation of VUV radiation upon reflection of a laser pulse of relativistic intensity from a plasma mirror [7]. In this case, the limitation on the laser pulse duration is relaxed compared to the case of generation in gases, since only one attosecond burst is generated in each cycle (unlike in a gas, the nonlinear medium is not centrosymmetric in this case). In the experiment, a 7-fs laser pulse with a controlled waveform was used; the peak intensity at the focus was slightly lower than 10^{18} W cm^{-2}. It is shown that the wavefront rotation leads to the appearance of spatial modulation in the generated VUV radiation, namely, several peaks separated in the directions of propagation appear, which can be interpreted as individual attosecond pulses.

In [104], the attosecond lighthouse technique was first implemented for HHG in a gas.

3. Methods for measuring attosecond pulses

With the development of technology for producing subfemtosecond pulses, the question arose as to the possibility of their characterization using techniques previously developed for the optical range. The question turned out to be difficult, since the carrier frequency of attosecond pulses falls into the VUV or soft X-ray frequency range, which is still insufficiently supported by metrology. One of the main difficulties is the lack of optical elements with the required characteristics for this range, which makes radiation transportation problematic. In addition, the nonlinear polarizabilities of substances rapidly tend to zero with increasing frequency of the incident radiation, which greatly complicates the implementation of various correlation measurement methods in the high-frequency region. The situation is further aggravated by the fact that the intensity of generated attosecond pulses is, as a rule, low, so that only in some cases, due to sharp focusing, is a level of 10^{14} W cm^{-2} reached [105, 106]. The low intensity level of the pulses to be measured does not yet allow efficient use of autocorrelation measurement methods based on the use of nonlinear properties of the medium (see Section 3.7 for more details). Therefore, the task of measuring attosecond pulses required a serious modernization of measurement methods known in optics, and even the development of fundamentally new ones. Most of the methods for measuring attosecond pulses are based on various modifications of such methods of pico- and femtosecond optics as a streak camera [107, 108], FROG (Frequency-Resolved Optical Gating) [109, 110], SPIDER (Spectral Phase Interferometry for Direct Electric field Reconstruction) [111], and tomography [112, 113]. Sections 3.1–3.7 briefly describe the main methods proposed so far for measuring attosecond pulses.

The attosecond radiation generated in the HHG process is ideally synchronized with the laser radiation that serves as a pump in this process [3]. Thus, to measure the characteristics of the generated attosecond radiation, one can use a part ('replica') of the initial laser radiation split off from the main beam and directed into the measuring chamber with a controlled delay. It is on this principle that most methods for characterization of attosecond pulses are based. This measurement technique, called cross correlation, uses the simultaneous action of attosecond radiation and a delayed replica of a laser pulse on a gas in the measuring chamber.

The widest group of attosecond metrology methods involves the use of spectroscopy of photoelectrons generated in the course of measurements. For this group of methods, an experiment on measuring the duration of an attosecond pulse is reduced to the following: a beam of UV radiation to be studied (which is a train of attosecond pulses or a single attopulse) and a beam of laser radiation coherent with it (below, we refer to it as a dressing field) are focused into a gas jet. The intensity of the dressing field is chosen so that it does not in itself cause gas ionization. There is a variable phase delay φ between the generating and dressing fields; thus, the position of the attopulses relative to the peaks of the instantaneous value of the low-frequency field is controlled. Photoionization of the gas is caused by an attopulse, and the action of the dressing field leads to a modification of the spectrum of emerging photoelectrons. Historically, the first proposed method for determining the duration of a single attosecond pulse is the attosecond streak camera [114]. However, a more detailed theoretical study (see Sections 3.1–3.7) shows that the energy and angular spectra of photoelectrons can provide much broader information. In general, methods such as FROG-CRAB, SPIDER (for somewhat more complex experimental conditions), and RABBIT (for an attosecond pulse train) are based on the same principle.

3.1 RABBIT method

The method for measuring attosecond pulses called RABBIT (originally abbreviated RABBITT, Reconstruction of Attosecond Beating By Interference of Two-photon Transitions) [15, 18, 115], unlike the other methods discussed below, has no direct equivalent in the optical range (although, as we will show later, it is actually a variant of optical gating). The RABBIT method is used when a train of attopulses with similar parameters is generated. The spectrum of such radiation is a set of odd harmonics; to reconstruct the time characteristics of attopulses, not only the intensity of the harmonics but also the phase difference between them must be known. In gas photoionization under the combined effect of harmonics and a low-frequency field of moderate intensity, the spectrum of photoelectrons contains not only peaks corresponding to absorption of a harmonic quantum but also additional peaks (sidebands) at frequencies of *even* harmonics corresponding to absorption of one harmonic quantum ± one quantum of a low-frequency field [116] (Fig. 6). Thus, the peak at the frequency of the even harmonic $2q\omega$ is associated with two processes, which can be denoted as $\omega_{2q-1}+\omega$ and $\omega_{2q+1}-\omega$ (here, ω_{2q-1} and ω_{2q+1} are the frequencies of neighboring odd harmonics). The probability amplitudes of these processes interfere constructively or destructively, depending on the delay τ, as well as on the phase difference $\varphi_{2q-1}-\varphi_{2q+1}$ between adjacent harmonics, so that the intensity of this peak is given by [116]

$$S_{2q}(\tau) \propto \cos\left(2\omega\tau + \varphi_{2q-1} - \varphi_{2q+1}\right). \tag{5}$$

(the argument in (5) in the general case also contains an additional term due to the complexity of the corresponding

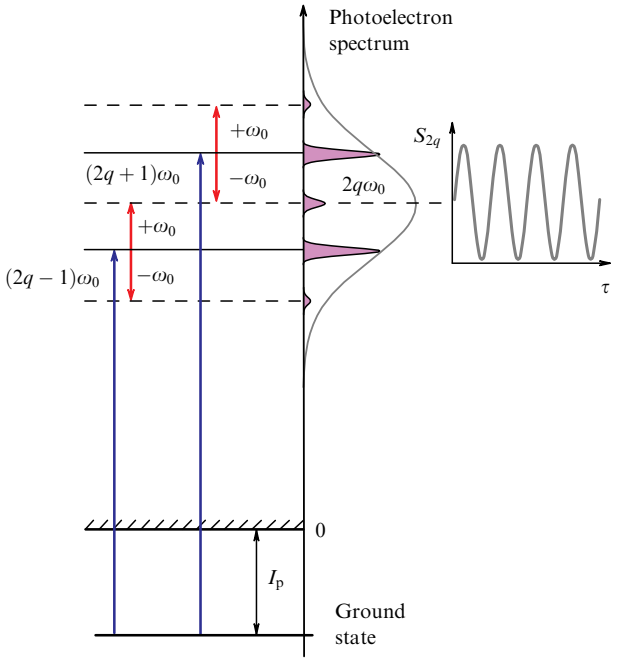

Figure 6. Explanation of the principle of measurement of phases of harmonics by the RABBIT method.

atomic matrix element, which is usually negligible or can be calculated theoretically (see Table 1 in [15])).

Thus, by measuring the dependences of the intensities of various peaks in the photoelectron spectrum on the delay time τ, it is possible to retrieve the phase difference between adjacent harmonics over the entire spectrum, i.e., total spectral distribution of the radiation phase. For successful application of the method, it is necessary that neighboring peaks in the photoelectron spectrum be well resolved, i.e., it is not applicable for measuring single attosecond pulses.

The RABBIT method was the first to experimentally measure not only the duration of an attosecond pulse but also its time profile [15]. The authors of [15] used a 40 femtosecond Ti:Sa laser pulse to generate high harmonics in an argon jet. The second jet of argon was used to diagnose the generated radiation in the range of harmonics from the 11th to the 19th. As a result of measurements, the authors obtained an average field profile of the attosecond radiation generated in this experiment, which was a sequence of pulses with a duration of 250 as each; the measurement error was about 20 as. This technique was developed in [16, 117] and used in a number of experiments [118–120]. The RABBIT method and the results achieved with its help are described in more detail in reviews [18, 121, 122].

In [123], the RABBIT method was used to study the phases of high harmonics generated in the plasma of a laser plume. It was shown that the phases of the harmonics generated in this medium are consistent with each other; the presence of resonance with the transition from the ground state of the generating particle to the autoionization state leads to a significant addition to the phase of the resonant harmonic, in accordance with theoretical calculations [124, 125].

3.2 Attosecond streak camera

The attosecond streak camera method, as its name implies, is an upgrade of the conventional streak camera. The basic principle of operation of a streak camera is the creation of an electronic replica of a light pulse as a result of irradiation of a photocathode and the measurement of the duration of the resulting electron pulse using electronic optics. The basic principle of measurement in the attosecond streak camera remains the same. An attosecond pulse creates photoelectrons through single-photon ionization of gas atoms, photoelectrons are accelerated by a dressing field, and then the angular or energy spectrum of photoelectrons is measured, which depends on how quickly photoionization occurred compared to the duration of the optical cycle of the accelerating field, i.e., on the duration of the attosecond pulse (Fig. 7).

Consider a photoelectron born with kinetic energy

$$W_0 = \frac{v_0^2}{2} = \Omega - I_\mathrm{p} \gg I_\mathrm{p}\,,$$

where Ω is the central frequency of an AP. (Here and below, the system of atomic units is used: $e = m = \hbar = 1$.)

After the end of the low-frequency pulse, the electron born at the instant t will have a final velocity (the laser pulse is rather short, so the displacement of the electron during the laser pulse is much smaller than the focus size) given by

$$\mathbf{v}_f = \mathbf{v}_0 - \frac{\mathbf{A}(t)}{c}\,, \tag{6}$$

where $\mathbf{A}$ is the vector potential of the field. Since the UV field has a high frequency and low intensity, the acceleration of a free electron by the UV field may be ignored and only the vector potential of the low-frequency field may be considered to be $\mathbf{A}$.

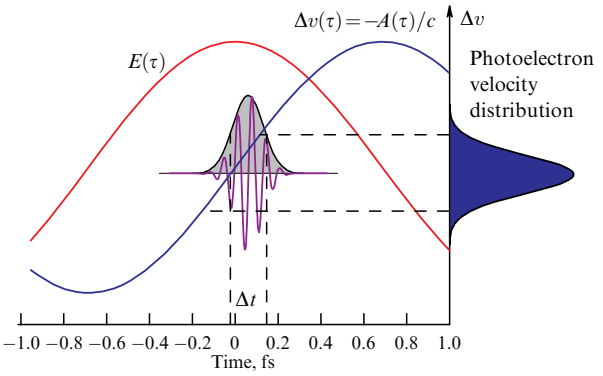

Figure 7. Explanation of the principle of measuring the duration of an attosecond pulse using an attosecond streak camera when registering photoelectrons in a parallel direction.

If the low-frequency field has a circular polarization, then the most probable direction of the electron final velocity is determined by the direction of the vector potential $\mathbf{A}(t)$ at the photoionization instant. Thus, by measuring the electron angular distribution after the end of the action of the deflecting field, one can calculate the duration of the incident attosecond pulse [114]. The error of this method depends on the value of the initial kinetic energy of electrons.

In [29, 126–128], a linearly polarized laser field, rather than a circular one, was used. The measured observable was not the angular but the energy distribution of electrons emitted at an angle θ to the polarization direction of the laser field, as a function of the delay time τ between the attosecond and laser pulses. From (6), one can find the electron energy after the end of the low-frequency pulse (we assume $A(t) \approx -[cE(t)/\omega]\sin(\omega t + \phi)$, where $E(t)$ is the slowly varying amplitude of the laser field) [126]:

$$\begin{aligned}\frac{v_f^2}{2} &= \frac{v_0^2}{2} + \frac{A^2(t)}{2c^2}\cos(2\theta) - \frac{A(t)}{c} \\ &\times \cos\theta\sqrt{v_0^2 - \frac{A^2(t)}{c^2}\sin^2\theta} \\ &\approx W_0 + 2U_\mathrm{p}(t)\cos(2\theta)\sin^2(\omega t + \phi) + \alpha\sqrt{8W_0U_\mathrm{p}(t)} \\ &\times \cos\theta\sin(\omega t + \phi)\,,\end{aligned} \tag{7}$$

where

$$\alpha = \sqrt{1 - \frac{2U_\mathrm{p}(t)}{W_0}\sin^2\theta\sin^2(\omega t + \phi)}\,.$$

The energy spectrum of photoelectrons is broadened for two reasons: first, the finite spectral width of an attosecond pulse $\Delta\Omega$ leads to a finite width of the initial electron energy distribution ΔW_0; second, the finite duration of the attosecond pulse Δt corresponds to the spread of the values of t in (7), leading to a corresponding broadening of the final energy distribution. Thus, the signal recorded by the attosecond streak camera contains information about the value of Δt, which can be retrieved by appropriate processing of this signal.

Below, we will consider the two simplest photoelectron registration geometries, namely, parallel to the electric field of the laser pulse and in the perpendicular direction.

Registration in parallel direction ($\theta = 0$). In this case, Eqn (7), taking into account the condition $U_p \ll W_0$, is transformed into the following:

$$\frac{v_f^2}{2} \approx W_0 + 2\sqrt{2W_0U_p}\sin(\omega t + \phi)\,. \tag{8}$$

It follows from (8) that the spectrum of photoelectrons is shifted along the energy axis by a value that depends on which phase of the laser field the attosecond pulse to be measured falls into. A spectrogram showing the dependence of the photoelectron spectrum on the delay time (streak spectrogram) is recorded in the experiment. To further extract information about the duration and chirp of the attosecond pulse, the experiment is simulated numerically, with the parameters of the attosecond pulse being adjusted so that maximum agreement with the experimentally measured electron streak spectrogram is achieved.

Registration in perpendicular direction ($\theta = \pi/2$). In this geometry, formula (7) reduces to

$$\frac{v_f^2}{2} \approx W_0 - 2U_p\sin^2(\omega t + \phi)\,, \tag{9}$$

i.e., the maximum in the photoelectron spectrum oscillates at twice the frequency of the laser field as the delay between the laser and attosecond pulses changes.

In the case of perpendicular registration, the shift of the photoelectron spectrum is accompanied by its broadening. The formula for the spectrum width can be obtained by calculating the difference between the kinetic energies W of electrons emitted at angles $\pi/2 + \Delta\theta$ and $\pi/2 - \Delta\theta$, where $\Delta\theta$ is the angular size of the electron detector:

$$\begin{aligned}\Delta W(t) &= W\left(\frac{\pi}{2} + \Delta\theta\right) - W\left(\frac{\pi}{2} - \Delta\theta\right) \approx \left[W\left(\frac{\pi}{2}\right)\right.\\ &\left. + \left|\frac{\mathrm{d}W}{\mathrm{d}\theta}\right|_{\theta=\pi/2}\Delta\theta\right] - \left[W\left(\frac{\pi}{2}\right) - \left|\frac{\mathrm{d}W}{\mathrm{d}\theta}\right|_{\theta=\pi/2}\Delta\theta\right]\\ &\approx 4\sqrt{2W_0U_p}\,|\sin(\omega t + \phi)|\Delta\theta\,.\end{aligned} \tag{10}$$

It can be seen from (10) that, with a change in the delay time, the width of the photoelectron spectrum experiences, in addition to shift (9), oscillations according to the law $|\sin(\omega t + \varphi)|$. The corresponding streak spectrogram for the case of an ultrashort pulse of the accelerating field is shown in Fig. 8. The duration of an attosecond pulse can be found according to the criterion of the best fit between the calculated and measured spectrograms.

Using the streak camera method with registration in the perpendicular direction, the duration of a single attosecond pulse of 650 as was found in [29] when krypton atoms were exposed to a laser pulse with a duration of about 7 fs. According to estimates, the measurement error was 150 as.

Each of the two geometries discussed above has its own advantages. It can be seen from a comparison of Eqns (8) and (9) that the shift of the photoelectron spectrum is larger for parallel detection, since the first degree of the laser field strength enters into (8), while it enters quadratically into (9). Thus, for measurements in the parallel direction, a laser field of lower intensity can be used, which reduces the noise in the measured signal caused by photoelectrons resulting from ionization by the low-frequency field.

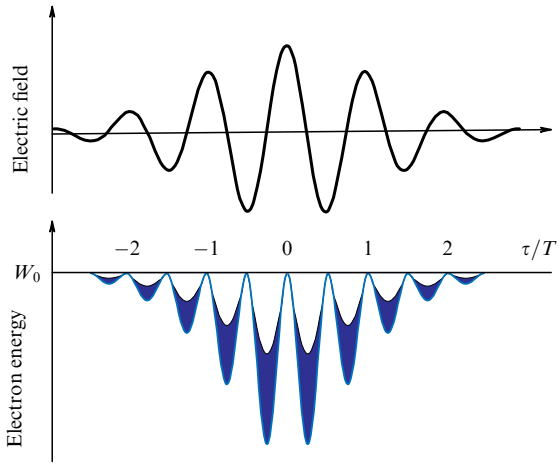

Figure 8. Explanation of the principle of measuring the duration of an attosecond pulse using an attosecond streak camera when registering photoelectrons in a perpendicular direction.

On the other hand, a shortcoming of the parallel registration scheme is that the energy shift introduced by the laser field depends on the initial electron energy. This dependence becomes significant if the spectral width of the electron wave packet is comparable to its average energy. The scheme with perpendicular registration is devoid of this drawback (see Eqn (9)).

The attosecond streak camera method described above is the simplest of all the methods presented in this review in terms of experimental implementation, but at the same time it provides only minimal information about the attosecond pulse under study. The methods presented below make it possible to extract more complete information about attosecond pulses.

The minimal duration Δt that can be measured with an attosecond streak camera is determined by the following condition: the change in the electron energy due to the dressing field is comparable to the uncertainty in the electron energy immediately after photoionization [53]. Under optimal conditions (with parallel detection and photoionization near the dressing field peak), this condition gives

$$\Delta t \propto \frac{1}{\sqrt{v_0E_0}}\,. \tag{11}$$

Formula (11) is only a rough estimate. At a high signal-to-noise ratio, the resolution of the method can be higher [30, 129, 130].

Note that the attosecond streak camera method does not imply mandatory stabilization of the absolute phase of the laser field. The attosecond streak camera method as well as other methods based on optical gating considered below are described in more detail in reviews [131–134].

3.3 Photoelectron spectrum with optical gating

Modulation of the photoelectron spectrum using a low-frequency field, which underlies the principle of operation of an attosecond streak camera, allows more complete measurements of both the attosecond UV pulse and the laser field itself. In this section, we present a general expression for the electron spectrum.

Let the field of an attosecond pulse have the form

$$E_X(t) = a_X(t)\exp(-\mathrm{i}\Omega t) + \text{c.c.} \tag{12}$$

It can be shown [126, 127, 135, 136] that the electron spectrum measured in the parallel direction with a delay τ between low-frequency laser and high-frequency attosecond pulses (as above, we assume that the high-frequency field is responsible only for photoionization, and the low-frequency field is only for acceleration after photoionization) can be written as

$$\sigma(v,\tau) = \left|d(v)\right|^2 \left| \int_{-\infty}^{+\infty} a_X(t)\, G(t-\tau) \times \exp\left[\frac{\mathrm{i}t(v^2 - v_0^2)}{2}\right] \mathrm{d}t \right|^2, \tag{13}$$

where

$$G(t-\tau) = \exp\left[\mathrm{i}\Theta(t-\tau)\right], \tag{14}$$

$$\Theta(t) = -v\int_t^{+\infty} A(t')\,\mathrm{d}t' - \frac{1}{2}\int_t^{+\infty} A^2(t')\,\mathrm{d}t', \tag{15}$$

v is the final electron velocity, and $d(v)$ is the dipole moment of transition from a bound state in an atom to a free state of an electron moving with velocity v. When deriving Eqn (13), it was assumed that this function is smooth (there are no resonances) and sufficiently 'slow', so that $d(v) \approx d(v + A(t))$. Note that the function $|d(v)|^2$ is usually known from independent experiments.

In the case of a very short attosecond pulse, the modification of the spectrum by a dressing field reduces to a shift [137] obtained in the classical treatment in Section 3.2. For a longer UV pulse, the modification of the spectrum is more complex [138–143]. Finally, for a train of attosecond pulses, the modification of the spectrum is the appearance of additional lines at frequencies of even harmonics, as discussed in the description of the RABBIT method.

As mentioned above, the use of such a method as an attosecond streak camera makes it possible to measure the characteristics of not only an attosecond pulse but also the laser field itself; moreover, in the attosecond streak camera method, the objects of measurement are no longer the cycle-averaged values, as in the methods of femtosecond optics, but the change in the laser field on a time scale within one optical cycle. Such measurements are carried out most directly when using a short single attosecond pulse with registration of electrons in the parallel direction; then, at a sufficiently high electron initial energy (determined by the average photon energy in the attosecond pulse), the shift of its energy as a result of the action of the laser field is proportional to the vector potential of the electric field of the laser pulse at the ionization instant (see the classical consideration in Section 3.2). In the case of a laser pulse with a stabilized absolute phase (or, more generally, with a stabilized waveform), the measurement of the electron kinetic energy spectrum as a function of the variable delay between the attosecond and laser pulses makes it possible to record the time profile of the electric field oscillations. The first demonstration experiment in which such a measurement was carried out is presented in [144]. The possibility of performing such measurements plays an important role in the development of such important areas in the physics of ultrafast processes as the controlled synthesis of waveforms of ultrashort optical pulses and their application to control electronic processes, attosecond spectroscopy, and petahertz electronics [145–148].

3.4 FROG-CRAB method

The structure of formula (13) for the photoelectron spectrum allows one to consider it a spectrogram of an unknown function $a_X(t)$ (i.e., the Fourier transform of the product of this function and the time window $G(t-\tau)$). In contrast to the time window in the standard FROG method developed in femtosecond optics, in this case the time window constitutes the phase gate rather than the amplitude one (see Eqns (14), (15)). Since the time window function changes significantly on the subfemtosecond scale, this makes it possible to measure subfemtosecond durations. The use of iterative algorithms previously developed for reconstructing femtosecond pulses [149] or created specifically for characterization of attosecond pulses [150–154] makes it possible to recover from the spectrum (13) measured for various τ the complex amplitude of the attosecond pulse $a_X(t)$ and the time dependence of the instantaneous value of the low-frequency field $E(t)$ (which, of course, implies stabilization of the absolute phase of the low-frequency field). The method was named FROG-CRAB (FROG for Complete Reconstruction of Attosecond Bursts) [119, 136, 150]. Due to the large amount of information contained in the spectrogram, the resolution of the method (at a high signal-to-noise ratio) can be significantly higher than that given by estimate (11). The FROG-CRAB method makes it possible in principle to reconstruct not only the parameters of one AP but also the parameters of each of the series of attopulses, although the latter implies stricter requirements for the signal-to-noise ratio in the spectrum. In the case of a train of a large number of APs, the spectrum in the regions between harmonics consists mainly of noise, and then measurements can only be made using RABBIT.

The FROG-CRAB method was first successfully used in [67], where, as a result of optimizing the experimental parameters, it was possible to obtain an almost Fourier limited isolated attosecond pulse with a duration of only 130 as, and in [96] this method was used to measure a single AP with a duration of 67 as obtained by polarization gating in a two-color laser field. The complete temporal reconstruction of the characteristics of an attosecond pulse train using the FROG-CRAB method was experimentally demonstrated in [155]. In particular, the extraction of information about both the envelope of the attosecond pulse train and the detailed structure of each pulse in the train, including information about the relative contributions of long and short trajectories and the value of the corresponding attochirp, was demonstrated.

Thus, FROG-CRAB is a very powerful method for reconstructing the shape of attosecond pulses, but it also has the disadvantage inherent in all the methods described above based on optical gating. Namely, the temporal resolution of the method is determined by the intensity of the low-frequency dressing field (for more details, see Section 3.2). As a result, the measurement of very short APs with a wide spectrum may require such a high intensity of the low-frequency field that it itself will lead to atomic ionization. As a consequence, the useful signal in the spectrogram will be noisy or even completely suppressed due to the signal caused by the electrons detached from atoms by the low-frequency field. In [156], a method was proposed for measuring attosecond pulses which makes it possible to circumvent this limitation.

To measure attopulses, it was proposed in [156] to use the same spectrograms but filtered in a special way; namely, from the entire data set, it is necessary to select, using spectral filtering, only the component oscillating with the frequency of the dressing field when changing the delay time, and the spectrogram obtained in this way should be used to reconstruct the parameters of APs. Further, as in the FROG-CRAB method, an iterative algorithm is used to find the AP parameters. Due to the spectral selection of the most informative part of the complete spectrogram data, it is possible to significantly increase the temporal resolution of the method at moderate dressing field intensities ($10^{11}-10^{12}$ W cm^{-2}). This method, called PROOF (Phase Retrieval by Omega Oscillation Filtering), makes it possible to measure significantly shorter pulses, with a duration of 20 as or even less. In [68], using the PROOF method, single pulses with a duration of about 53 as obtained by the polarization gating method were measured. Note that, since PROOF involves the use of a low-intensity dressing field, with which the dominant contribution to the spectrogram is made by transitions involving only one IR photon in addition to the harmonic photon, this method is in a certain sense close to the RABBIT method but is intended for measuring isolated attosecond pulses.

3.5 SPIDER method

SPIDER (Spectral Phase Interferometry for Direct Electric-field Reconstruction) is, like FROG, a powerful method for measuring femtosecond pulses in optics. The advantage of SPIDER is that the algorithm for pulse reconstruction from experimental data is purely analytical, i.e., does not require the use of iterative procedures. In addition, the experiment requires measurement not of a spectrogram but of just one spectrum. The method is based on the interference of two replicas of the pulse to be measured, slightly shifted relative to each other in time and frequency. Let $E(\omega)$ be the Fourier transform of one of the replicas. Then, the Fourier transform of the replica shifted in time by τ and in frequency by ω' is expressed as $\exp(\mathrm{i}\omega\tau)E(\omega-\omega')$. Both replicas are sent to the input of the spectrometer. The resulting interferogram has the following form:

$$S(\omega) = \left|E(\omega) + \exp(\mathrm{i}\omega\tau)E(\omega-\omega')\right|^2. \qquad (16)$$

From this, the field of the initial pulse is analytically reconstructed in a unique way [111, 157].

The difficulty in implementing this method for attosecond pulses is how to change the frequency of one of the replicas. In optics, this problem is solved by mixing both replicas with two different parts of a long chirped pulse, differing in frequency by the value ω', in a nonlinear crystal. It is impossible to implement this mechanism in the case of attosecond pulses, since, as noted above, the nonlinearities in the corresponding frequency range are extremely low, and the intensity of attosecond pulses is not high enough. To date, several modifications of the SPIDER technique have been proposed for measuring attosecond pulses.

In [158], a measurement scheme based on the optical gating described above was proposed. Two replicas of an attosecond pulse shifted only in time create, as a result of gas photoionization in the presence of a dressing laser field, two electron wave packets shifted not only in time but also in energy, since photoionization occurs at different phases of the dressing field. An important advantage of this method compared to those described above is that much lower dressing field strengths are required, so the assumption that it does not perturb the photoionization process is quite reliable. Applying the standard SPIDER reconstruction procedure to the photoelectron spectrum, one can reconstruct the time profile of the electron wave packet and from it, the field of the initial attosecond pulse. The shortcoming of this scheme is that the measured quantity is the photoelectron spectrum, and the resolution (in terms of energy) of today's electronic spectrometers is still not enough to ensure the accuracy of spectrum registration required in this case.

The authors of [159] proposed generating two replicas of an attosecond pulse at once, which are slightly different in frequency. In this case, the classical purely optical SPIDER scheme is implemented, in which the recording element is a conventional X-ray spectrometer with a resolution much higher than the energy resolution of an electron spectrometer. To generate two replicas of an attosecond pulse, it is proposed to use two femtosecond pulses slightly shifted (by about 1% or even less) in frequency. The frequency shift of attosecond pulses will be much higher (approximately as many times as the central frequency of the AP is greater than the frequency of the generating field), which provides the desired value of the frequency shift. The fact that the shift of attosecond radiation is a function of the frequency of its spectral components, instead of being a constant value as in the classical SPIDER scheme, does not complicate the standard procedure for reconstructing the pulse field. The weak point of this approach is that the generating gaseous medium is partially ionized by the first femtosecond pulse and does not have time to recover by the time the second pulse arrives. To solve this problem, the authors of [159] proposed that the temporal separation of the pulses be replaced with the spatial one, which makes it possible to get rid of the aforementioned undesirable effect, and the SPIDER reconstruction procedure can be easily modified for such a configuration of the experimental scheme.

In [160], the results of the first experiment using the SPIDER technique with two laser pulse replicas spaced apart in time are presented, and the time profile of the 11th harmonic is also measured.

Obviously, the experimental implementation of the SPIDER method is rather complicated. However, for measuring durations much shorter than the optical cycle, this method is among the preferred ones. Its temporal resolution is determined by the accuracy of control over the time delay between the replicas of the field to be measured, as well as between these replicas and the peaks of the dressing field. It is important that attosecond pulses generated in two successive half-cycles of the laser field can be used as replicas [158, 161]. Since, as noted above, the dressing field is coherent with the generating one, the accuracy of control over these delays can be very high.

3.6 *In situ* measurements

The attosecond metrology methods described above belong to the class of *ex situ* methods, in which attosecond pulses are generated and measured in different gas targets. An alternative to this approach is *in situ* measurements carried out in the same medium in which high harmonics are generated. The *in situ* approach, in contrast to *ex situ* ones, makes it possible to measure the characteristics of attosecond pulses directly in the process of their generation. In [162], for such measurements, it was proposed to add a weak field at the second

harmonic to the generating laser field. Due to the low intensity of the field at the second harmonic, it has a significant effect only on the dynamics of free electrons. Thus, the instants of the release of an electron from an atom or molecule and its recombination effectively limit the perturbation in time, thereby creating a temporal mask. The field of the second harmonic breaks the initial symmetry of the process of ionization of particles of the medium, leading to the appearance of even harmonics. The intensity of these harmonics is maximum when the maximum of the field of the second harmonic overlaps to the greatest extent with the time interval of the free motion of the electron. By analyzing the spectrum of high harmonics as a function of the delay time between the fundamental radiation and its second harmonic, it is possible to reconstruct the parameters of the attochirp, which largely determines the time profile of the field of generated attosecond pulses. It is easy to see that, conceptually, this method is very close to the RABBIT method.

Since the method described above implies the breakdown of the symmetry of the temporal dynamics of the underlying high harmonic generation process between the adjacent half-cycles of the laser field, its direct use cannot provide an adequate measurement of isolated attosecond pulses. To eliminate this shortcoming, a slight modification of the method was proposed in [163]. Instead of using collinear beams, it was proposed to send the beam at the second harmonic at a small angle to the fundamental laser radiation. As a result, the phase shift between the components at frequencies ω and 2ω in the region of the laser focus turns out to be dependent on the vertical coordinate. As a consequence, the phase of the harmonic radiation also becomes changing in the vertical direction. The temporal breakdown of the symmetry of the harmonic generation process is then replaced by a spatial one, since the wavefront of the generated radiation is distorted under the influence of the second harmonic field. By measuring the angular distribution of the harmonic signal in the far zone at various delay times between the fundamental radiation and its second harmonic, one can obtain a complete analog of the spectrogram used in the FROG-CRAB method to retrieve the attosecond pulse parameters. A similar iterative algorithm is used here to retrieve the AP parameters. This method is called STRAP (Space-Time Reconstruction of Attosecond Pulses).

The advantage of *in situ* methods is that they require only measurement of the spectrum of the generated signal and not the electronic replicas of the attosecond pulses, i.e., these methods are purely optical. However, they also have significant drawbacks due to the fact that the measurement is inextricably coupled to the very process of generation of attosecond radiation. First, the *in situ* methods are based on the use of the second harmonic as a weak perturbation; therefore, they can only be used to characterize radiation generated in a single-color field. Second, if after the generation process the attosecond pulse is further modified in some way (for example, the attochirp is eliminated in a dispersive medium), then the measurement of the resulting pulse will require the use of standard *ex situ* methods. The pros and cons of *in situ* measurements are described in detail in review [164].

3.7 Autocorrelation methods

Although the vast majority of attosecond pulse measurements today use the principle of optical gating, recently, due to an increase in the intensity of the produced attosecond pulses, experiments beyond this approach have become possible.

To date, methods for measuring the autocorrelation function of a laser pulse using second-order nonlinear processes have been well developed. In measurements in the UV range, two-photon ionization of atoms can be used as a quadratic nonlinearity, namely, the yield of photoelectrons or ions, depending on the time delay between two replicas of a UV pulse, characterizes its autocorrelation function. In the case of UV radiation, due to the absence of nondispersive beam splitters used for the optical range, to implement a variable delay, wavefront splitters are used, which are a spherical mirror divided into two parts, one of which is fixed in space, and the other is shifted using a piezo-electric translator. According to estimates, the minimum intensity of UV radiation required for reliable detection of a nonlinear ionization signal is higher than 10^{10} W cm^{-2} [134]. Obtaining such an intensity or even higher ones is possible, for example, due to the spatial focusing of high harmonics [21, 22, 165]. The described autocorrelation method was proposed and used to measure femtosecond [166] and then subfemtosecond [17, 167–169] UV pulses both in the form of a train [17, 167, 168] and in the form of a single AP [169, 170]. In addition, the use of this nonlinearity made it possible to carry out an even more complete reconstruction of the attosecond pulse, namely, in [171], an almost complete analog of the optical FROG method was implemented. In experiment [171], the spectrum of photoelectrons was recorded as a function of the delay time τ between two replicas of an attosecond pulse $E_X(t)$:

$$\sigma(W,\tau) = \left| \int_{-\infty}^{+\infty} E_X(t) E_X(t-\tau) \exp(\mathrm{i}Wt)\,\mathrm{d}t \right|^2, \qquad (17)$$

where W is the photoelectron energy. It can be seen that this spectrogram is formally identical to the FROG spectrogram when this method is used for femtosecond pulses. A similar approach was proposed in [172] for measuring the characteristics of an AP train.

The methods described above in this section are based on the use of a nonresonant two-photon photoionization process. The use of *resonance* processes makes it possible to significantly (by orders of magnitude) relax the requirements for the UV radiation intensity. In [173–175], a method based on resonant excitation and subsequent dissociation of excited molecules was proposed. It is also possible to use resonant two-photon excitation of a high-lying autoionization state; photoexcitation of an autoionization state of a helium atom using a combination of the 19th and 21st harmonics of a Ti:Sapphire laser was addressed in Ref. [176]. With the help of approaches [173–176], the UV field can be analyzed, but in a relatively narrow spectral range determined by the energy of the excited state. The ART method (Attosecond pulse Reconstruction using Raman-type Transitions) [177], which is based on the use of two-photon *Raman* transitions, is free from this shortcoming, since, for such transitions, the energy of a UV photon can be significantly higher than that of an excited level.

Among the advantages of using resonance processes is also the relative ease of registration, since measuring the efficiency of molecular dissociation or that of the photoexcitation of atoms is much simpler than measuring the photoelectron spectrum. In [177], a completely optical version of the method for measuring the autocorrelation of attosecond pulses was also proposed.

The methods described in Sections 3.1–3.6 require the use of nonlinear interactions of light with matter. In addition, all these methods require a series of measurements at different delays between the components of the used multicomponent light fields and are highly sensitive to noise. In [178–180], an all-optical method of 'double-blind holography' was developed, based on linear measurements of the spectra of two unknown ultrashort pulses and their spectral interference. The implementation of this method was demonstrated in [180] using attosecond pulses of harmonics generated in two different gases and in their mixture as an example. The feasibility of a reconstruction procedure based on a single measurement over a pair of attosecond pulses delayed relative to each other is also demonstrated, which makes it possible to apply this approach in the future in cases where the generated ultrashort pulses have a low repeatability (which is typical, for example, for pulses generated by free-electron lasers).

Some other methods for measuring attosecond pulses and new algorithms for their characterization are presented in [133, 134].

4. Applications of attosecond pulses

The creation of technologies for producing attosecond pulses has become a new stage in the development of experimental physics and the chemistry of ultrafast processes. The use of attosecond pulses has provided a number of fundamentally new possibilities for studying light-induced processes in matter and controlling these processes.

4.1 Attosecond probing of electronic processes

Attosecond spectroscopy has become one of the most rapidly developing areas of attosecond physics. Among the approaches to spectroscopic measurements with subfemtosecond time resolution, the most natural approach seems to implement the 'attosecond pump–attosecond probe' principle. However, due to the insufficiently high intensity of attosecond pulses currently available and the low efficiency of nonlinear processes in the VUV and X-ray ranges, this approach has not yet received significant development. The main approach exploited in attosecond spectroscopy, which is also implemented, in particular, in such methods of attosecond metrology as the attosecond streak camera [53, 126] and RABBIT [15, 181] described in Section 3, as well as in attosecond absorption spectroscopy [182, 183], is a mixed type, in which one of the pulses (pump or probe) is an attosecond pulse (or train of pulses) of VUV or X-ray radiation, and the other is an intense femtosecond laser pulse in the optical range from the same source that was used to produce attosecond pulses, synchronized with the first of the above. Important from the point of view of time resolution in this case are the duration of the attosecond pulses and the accuracy of control over the CE phase of the laser pulse and its delay relative to AP. Taking into account the existing achievements, it can be stated that time measurements with a resolution of several ten attoseconds are now becoming available, which has already been demonstrated in experiments [184].

4.1.1 Attosecond photoelectron spectroscopy. *Attosecond streak camera.* The time dependence of the ionization currents arising from the emission of primary photoelectrons due to the single-photon photoelectric effect largely repeats the time profile of the attosecond pulse intensity. In the case of an AP with a duration much shorter than the cycle of the dressing laser field, the profile of the streak spectrogram will be oscillations repeating those of the vector potential of the dressing field and broadened in accordance with the spectral width of the attosecond pulse. The emission of secondary electrons (arising, for example, as a result of the Auger process) can have a characteristic duration comparable to or even exceeding the laser field cycle. In this case, interference modulations appear in the resulting streak spectrogram, the interpretation of which (for example, by comparison with the results of theoretical modeling) allows one to extract information about the dynamics of the corresponding secondary process. The first example of such observations was the use of an attosecond streak camera to measure the time of the Auger process in krypton atoms [185]. The measured lifetime of a vacancy in the M shell of the Kr atom was about 7.9 fs.

Another important aspect of the dynamics of ionization processes is the time delay of ionization. The theory of ionization processes relates this quantity to the so-called Wigner delay, first introduced by Eisenbud, Wigner, and Smith [186–188] when considering the problem of electron scattering by a potential well. The Wigner delay, defined in the scattering problem as the derivative of the scattering phase with respect to particle energy E, is interpreted as the delay time of the wave packet scattered by the central potential. Since ionization can be considered a special case of scattering, the theory of ionization processes also introduces a quantity analogous to the Wigner delay, which is interpreted in this case as a time delay between the light pulse and the emission of an electron.

Experimental studies of photoionization delays became possible with the advent of techniques for producing pulses with a duration of less than 100 as. One of the first such studies in atomic gases was the measurement of the delay time between the instants of ionization from different electronic states (2s and 2p states in neon) [184]. The delay found was 20 as, which at that time was a record short time interval measured in observations of microscopic processes in matter. The measurements carried out stimulated the development of a new direction in attosecond physics related to the study of the inertia of ionization processes. Such studies are of great interest both from a fundamental point of view and in the context of solving the 'zero time' problem in attosecond measurements. Numerous theoretical studies on this problem have revealed that theories that take into account the effect of many-electron correlations on photoionization, as a rule, give a much shorter time (~ 5 as) for the Wigner ionization delay than what the results of experimental observations give for these delays. Significant discrepancies with the experimental results called into question both the accuracy of the theories of photoionization of complex atoms and the limits of applicability of the approximations (primarily the strong-field approximation) underlying the analysis of measurement data obtained with the attosecond streak camera. The results of theoretical and experimental studies in this area are given, in particular, in review [189] and the literature cited therein. It was found, in particular, that a significant contribution to the delay experimentally measured by the attosecond streak camera is made by artifacts not related to the Wigner delay, such as the effect of the Coulomb field of the parent ion on the motion of a free electron under the action of a probing laser field and the laser-induced polarization of the atom under study.

Improving the experimental setup using an attosecond streak camera made it possible to carry out measurements that shed light on the role of many-electron interactions in the photoelectric effect [190]. The object of research was the helium atom, which is the simplest multielectron system for which exact numerical quantum mechanical calculations can be made; the results of the experiment were compared with the corresponding numerical calculations, which made it possible to extract from the processing of experimental data high-precision information about the delay times between different photoemission channels, namely, the direct detachment of an electron and the process in which part of the energy of the absorbed VUV photon is carried away by the released electron and the other part is spent on the excitation ('shaking-on') of the second atomic electron. Measurements with different energies of the VUV photon made it possible to obtain detailed information on the process of intra-atomic energy redistribution due to inter-electron correlations. For the first time in attosecond physics, the accuracy of time delay measurements reached the subattosecond level (down to 850 zeptoseconds).

Although initially the main object of research related to the application of attosecond pulses was gaseous media, the principle of an attosecond streak camera is also increasingly used to study electronic processes in solids. In the first demonstration experiment [191], the process of charge transfer in a tungsten crystal was studied. Comparing spectrograms from electrons removed by an attosecond pulse from deep levels and from the region near the Fermi surface made it possible to obtain a value of ~ 110 as for the delay time between the emission of electrons localized near nuclei and delocalized electrons closer to the conduction band boundary, which gives the corresponding time scale of electron transport in tungsten. In sharp contradiction to the results of measurements in tungsten, similar measurements in magnesium [192] did not reveal (within the experimental accuracy of ~ 20 as) differences between the instants of emission from the surface for initially deeply localized electrons and delocalized electrons of the valence band. The results obtained in [192] indicate that the initial degree of electron localization is not the only and, perhaps, not the most important factor determining the dynamics of photoemission in solids; a much more important role can be played by the characteristics of the substance (the energy dependences of the group velocities of electron wave packets and their mean free paths) that govern the transport of electrons. The demonstrated capabilities of attosecond photoemission spectroscopy will undoubtedly find further application in studies on natural time scales of electronic processes of charge dynamics in solids and on surfaces.

Photoelectron interferometry. This group includes methods in which information about the processes under study is extracted from observations of the interference modulation of the photoelectron spectra and its changes when the delay time between the initially synchronized VUV and IR radiation pulses is varied. As the VUV field, both isolated attosecond pulses and their trains, both obtained from HHG driven by an IR field, can be used.

As an example of the use of single attosecond pulses, we point to the interferometric method demonstrated in [193] for measuring the characteristics of electron wave packets (EWPs) of bound states excited when atoms or molecules are exposed to a single attosecond pulse. Attosecond radiation is chosen so that its spectral composition makes it possible to simultaneously excite the EWP of both bound and continuum states. The EWP of bound states is used as a reference signal, and probing is provided by an IR pulse, which is directed into the medium with a controllable delay relative to the attosecond pulse and causes additional ionization of gas particles. The EWP of continuum states created by direct (VUV) and two-stage (VUV + IR) ionization interfere; processing of the interferogram obtained when measuring the spectra of photoelectrons at different relative delays of the VUV and IR pulses makes it possible to extract information about the spectral composition of the EWP of bound states. In this case, the spectral resolution is determined by the reciprocal of the VUV/IR delay and turns out to be hundreds of times higher than the value determined by the width of the Fourier spectrum of the exciting (attosecond) pulse.

As one of the areas of research based on the use of sequences of attosecond pulses (RABBIT, etc.), we note measurements of the dynamics of photoemission processes, carried out by observing and processing the interference component in the spectrum of emitted electrons when the medium under study is exposed to a train of VUV pulses and a replica of the IR pulse used to produce this AP train. One of the first experimental studies that demonstrated the feasibility of measuring the time delay between the instants of ionization from different electronic states using the interference technique was presented in [194]. The measurements in [194] were based on a comparison of the spectrograms from free electrons obtained as a result of ionization from the 3s and 3p states of argon under the action of high-harmonic radiation in the presence of an additional weak field at the fundamental frequency with a variable time delay.

We also note studies that demonstrated the effect of atomic [195] and molecular [196, 197] resonances on the phase shifts of the modulation of certain components of the photoionization signal in the RABBIT method. As an example of experimental observations of such effects, it is worth noting study [198], where photoionization delays associated with the influence of shape resonances for the N_2O molecule were measured. Such resonances are observed when the effective potential, which is the sum of the molecular and centrifugal potentials, forms a trap in which metastable states arise; the capture of a photoelectron in a trap causes a delay in its detachment from the molecule. In the energy range from 20 to 40 eV addressed in [198], several shape resonances corresponding to different electronic states were revealed; the maximum measured delay, mainly due to these resonances, was about 160 as.

The original version of the RABBIT method involved the analysis of energy-integrated oscillations of additional maxima in the spectra of photoelectrons. However, the high spectral resolution of modern electron spectrometers makes it possible to carry out such measurements with energy resolution. The corresponding technique, called Rainbow RABBIT [199, 200], makes it possible to measure changes in the spectral amplitudes and phases of a recorded signal within a single additional peak. Such changes can be significant when the continuum of energy states of an atom or molecule in a given energy range has a sharp structure, which is observed, for example, in cases corresponding to autoionization states, shape resonances, Cooper minima, etc. Measurements provided by the Rainbow RABBIT method make it possible to determine the relative contributions of various ionization processes to the recorded signal or to analyze complex electronic wave packets.

4.1.2 Attosecond absorption spectroscopy. Recently, Attosecond Transient Absorption Spectroscopy (ATAS) has become one of the powerful methods of experimental research in attosecond physics [182, 193, 201]. Unlike the methods presented above, ATAS is completely optical; namely, it is based on the observation of changes in the integrated or spectrally resolved absorption of the energy of an attosecond pulse when its delay is varied with respect to a femtosecond laser pulse synchronized with it. The optical registration system used by the ATAS method is attractive in that it is technically much simpler than the approach underlying attosecond photoelectron spectroscopy methods, which require the measurement of electron spectra. Moreover, the technique of attosecond transient absorption does not impose serious restrictions on the intensity of laser radiation and can be successfully used both at low intensities, when the ionization probability and ponderomotive energy of electrons are not high enough to provide acceptable signal levels and energy resolution of photoelectron spectroscopy methods, and at high intensities, when the appearance of a large number of additional ionization channels makes it difficult to interpret the electron spectra. An important advantage of X-ray spectrometers used in attosecond absorption spectroscopy is their high spectral resolution, which is necessary for detecting subtle changes in the transmission spectra of the media under study [202]. Unlike attosecond photoelectron spectroscopy, the ATAS method makes it possible to simultaneously observe the dynamics of states lying both above and below the ionization threshold.

The ATAS method implies two main scenarios that differ in the order in which IR and VUV pulses are sent to the target. In a more traditional scenario (IR→VUV), the medium is first exposed to an IR pulse, which excites one dynamic process or another in it. This process is probed by an attosecond VUV pulse sent with a variable delay τ. In this case, information about the dynamics of the process under study is contained in the delay-dependent integrated or photon energy-resolved intensity of the VUV radiation transmitted through the medium (Fig. 9). In another scenario (VUV→IR), which seems less logical, the attosecond pulse affects the medium before the peak of the IR pulse (or overlaps with this peak). In this case, the attosecond pulse serves as a pump, which, due to its large spectral width, excites the internal atomic, molecular, or ionic dynamics involving a large set of energy states (or, in other words, creates the polarization of a quantum system), while IR radiation, acting on this system, changes these dynamics via coupling, by means of one- or multi-photon transitions, of the states of the excited system with other states of the discrete or continuous spectrum (or, in other words, perturbing the polarization created by the attosecond pulse). The dynamics of all processes occurring during such a two-pulse action are reflected in the observed VUV absorption spectrogram. The structures observed in the transmission spectra of VUV radiation passing through the medium under study can be interpreted as the result of spectral interference between the radiation emitted by an excited system and the broadband radiation transmitted through the medium. The perturbation of the induced polarization by an IR pulse changes the resulting spectral structure of the observed radiation (Fig. 10) [203].

The first application of the ATAS method using a single AP, in which the IR→VUV scenario was implemented, was

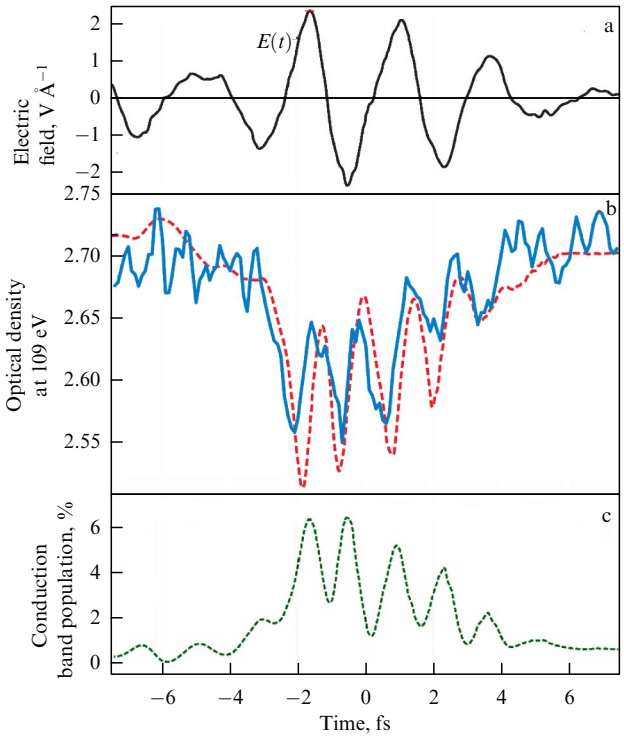

Figure 9. Results of observations of ultrafast reversible insulator–conductor transitions during the action of ultrashort Ti:Sapphire laser pulses on a dielectric (silicon dioxide) using attosecond absorption spectroscopy. (a) Time profile of the electric field of the laser pulse measured by the attosecond streak camera method, as functions of the delay time between a 72-attosecond probing AP and the laser pulse. (b) Optical density of the SiO_2 sample near $\hbar\omega_0 = 109$ eV, integrated over the interval $\Delta\hbar\omega_0 = 1$ eV (solid curve: data from experimental measurements, dashed curve: result of theoretical calculations). (c) Population of the conduction band (theoretical calculation). (Taken from Ref. [204].)

demonstrated in [182]. The dynamics of a wave packet of bound electronic states created as a result of ionization of krypton atoms by a few-cycle laser pulse with stabilized CE phase were studied. The spectrogram of absorption of an attosecond pulse by Kr^+ ions, constructed from 40 absorption spectra measured at various delays with a step of about 1 fs, made it possible to retrieve the dynamics of oscillations of the spatial charge distribution (including the hole formed due to ionization of the Kr atom) within the 4p shell with a period of about 6 fs. The ATAS technique using a train of attosecond pulses was first demonstrated in [183], where oscillations of the transmission of photons of various harmonics were observed, which are caused by the interference of electron wave packets when helium atoms are exposed to a superposition of a laser pulse and the AP train generated by it.

Within the framework of the approach described above, using a single AP, observations of laser-induced dynamics in solid media were also carried out. For instance, ultrafast reversible insulator-conductor transitions were observed in Ref. [204] during the action of few-cycle pulses of a Ti:Sapphire laser on a dielectric (SiO_2) (see Fig. 9). The demonstrated control of the conductivity of solid media on the scale of one cycle of the laser field (less than 3 fs) indicates the prospects for advancing the speed of optoelectronic devices to the petahertz regime [147], which is several orders of magnitude faster than the speed of today's semiconductor electronics.

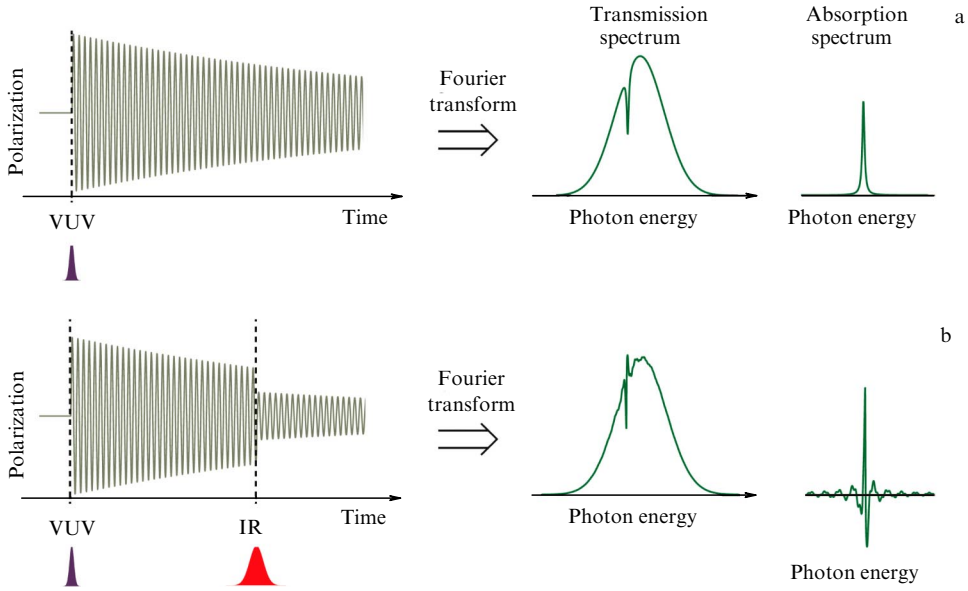

Figure 10. Explanation of the principle of attosecond absorption spectroscopy when an attosecond pulse precedes the peak of the IR pulse. (a) Sample is exposed only to the VUV field. Attosecond VUV pulse induces polarization in the sample (left); photons re-emitted in this case are added, with a certain phase delay, to transmitted photons; spectrum of the full transmitted signal (center) contains a dip near the resonant transition frequency; it corresponds to a single peak in the absorption spectrum (right). (b) IR pulse irradiating the medium with some delay perturbs the induced polarization (left), changing the spectrum of the transmitted signal (center) and modifying the observed absorption profile (right). (Taken from Ref. [203].)

The second (VUV→IR) scenario described above has been widely used in experimental studies of a wide variety of ultrafast processes in matter. In particular, studies of the dynamics of such phenomena as electromagnetically induced transparency [205], the dynamic Stark effect [206], and quantum beats between excited atomic states [207, 208] were carried out in real time using femto- or attosecond VUV radiation produced by HHG. The possibility of observing various short-lived states, such as autoionization [201, 209] and light-induced [210, 211] states, and studying their dynamics is shown. For example, studies in Refs [210, 211] demonstrated the probing of the transient dynamics of absorption of VUV radiation (in the form of a single attosecond pulse) in helium atoms in the presence of an ultrashort IR laser pulse. In the measurements, transient structures in absorption were observed, which are manifestations of laser-induced virtual intermediate states (Light-Induced States, LISs) arising in the processes of two- and three-photon absorption of a two-color (VUV + IR) field.

The results of experiment [210] are shown in Fig. 11. In the region of overlapping of VUV and IR pulses marked with a red rectangle, structures are observed due to two-photon processes involving LISs. In experiment [211], oscillating structures near the single-photon ionization boundary were also clearly observed, corresponding to a time-resolved (and proportional to the instantaneous intensity of the IR field) shift of the continuum boundary in the energy spectrum of an atomic valence electron (the magnitude of which, averaged over the field cycle, is well known as the ponderomotive shift of ionization threshold [212]).

Soon after the first experiments with atomic gases, the ATAS method began to be used to study various ultrafast processes in molecules. The first results of these studies are presented in [213–216]. The development of HHG-based compact sources of soft X-rays (including pulses of attosecond duration) with photon energies in the 'water window' region (from 284 to 543 eV, i.e., between the edges of the

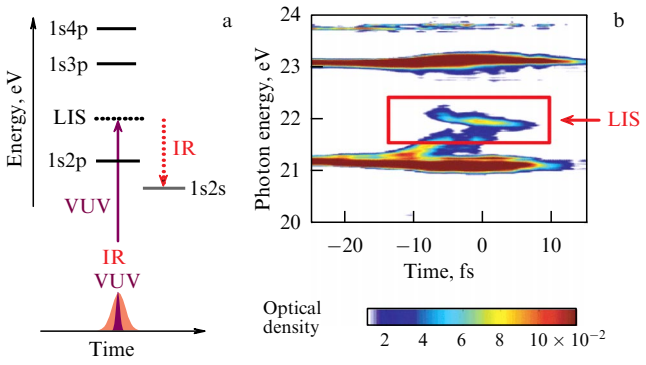

Figure 11. Observation of light-induced states (LISs) by attosecond absorption spectroscopy. (a) Energy level diagram showing LIS in helium. Solid purple arrow represents the VUV photon, and dotted red arrow represents the IR photon. Levels to which one-photon transitions from the ground state are allowed are shown by black horizontal lines; solid gray line is for 'dark' states and dotted black line is for LISs. (b) ATAS spectrogram. For negative time delays, the VUV pulse precedes the IR pulse. For large negative and positive time delays, only absorption peaks corresponding to allowed one-photon transitions are observed. In the region of overlap between VUV and IR pulses (near zero delay), highlighted by the red rectangle, structures due to LISs are observed. (Taken from Ref. [210].)

K-absorption bands of carbon and oxygen) (see [217] and the literature cited therein) opened wide possibilities for using femto- and attosecond X-ray absorption spectroscopy for element-specific studies of the dynamics of processes in complex molecules [218–221], including those in such environments as solutions [222, 223] and surfaces. For example, the use of single attosecond pulses with a spectral distribution maximum near 400 eV, i.e., near the edge of the nitrogen K-absorption band, made it possible to simultaneously study the attosecond electronic, femtosecond vibrational, and subpicosecond rotational dynamics of the NO molecule using ATAS [221].

Although in attosecond experiments in the framework of the pump–probe scheme an intense laser pulse in the optical range is used as one of the pulses that act on the object under study, theoretical studies also discuss possible experimental methods in which only attosecond pulses could be used. A scheme of this type was proposed, for example, for probing the dynamics of the appearance and evolution of vacancies created on inner atomic shells by attosecond radiation [224]. According to the proposed scheme, a vacancy is created as a result of ionization from the inner shell under the action of an attosecond pulse, and probing is carried out by an attosecond pulse with a central frequency in resonance with the frequency of the transition between an occupied deep-lying level and a vacancy.

4.2 Attosecond initiation of intraatomic and intramolecular processes

The study of intraatomic and intramolecular processes initiated by attosecond pulses has become an important branch of attosecond physics. Typical in this case is a mechanism in which, due to the large photon energy and the short duration of the attosecond pulse, at a well-defined point in time, the system is transferred to some transient excited state, after which its dynamics are determined by the action of the field of an intense laser pulse in the optical range.

As applied to atomic systems, such an approach was first demonstrated in [225]. An attosecond pulse with a central photon energy of about 91 eV acting on neon atoms initiated single-photon ionization from the 2p state. In this case, transitions from deep to higher levels occurred with a certain probability in the emerged Ne^+ ions as a result of electron 'shaking-on' (transfer of excess energy when a valence electron is detached by an attosecond pulse). Next, the gas target was exposed to a femtosecond IR pulse with a variable delay. Under the action of this pulse, tunneling ionization of Ne^+ ions appeared. Measuring the yield of doubly charged ions as a function of the delay time between the pump (VUV) and probe (IR) pulses made it possible to resolve in time the dynamics of the process described above. A stepwise increase in the yield of Ne^{2+} ions was observed from one half-cycle of the laser field to another with a probability depending on the instantaneous amplitude of the laser pulse. In the experiment with neon atoms, a time of 380 as was obtained for the two-stage process of populating the excited states of the Ne^+ ion and tunneling from them.

One of the first implementations of this scheme for molecular systems was the experimental study of the dissociative ionization of the H_2 molecule and the dynamics of the nuclear wave packet of the emerged H_2^+ molecular ion under the action of attosecond VUV pulses of high harmonics and femtosecond radiation at the fundamental frequency [226]. As demonstrated, the yield of dissociation products and the spectrum of their kinetic energies strongly depend on the duration of the laser pulse and its delay relative to the AP, which, notably, indicates the feasibility of attosecond control over the processes of light-induced dissociation of molecules.

The scheme described above was developed in the experimental study [227], in which the dynamics of electron localization as a result of attosecond photoionization of a molecule were studied. Thus, single attosecond pulses were first used to probe intramolecular electron dynamics. As a result of the research, it was shown that, in dissociative ionization of a hydrogen molecule, the localization of an electron exhibits subfemtosecond time-scale dependence on the delay time between the VUV and IR radiation pulses.

In [228], the application of the methodology developed in [227] to the study of ultrafast charge migration processes in more complex molecules was demonstrated. In the experiment, an attosecond pulse initiated fast ionization of the phenylalanine molecule. The subsequent action of a femtosecond probing laser pulse resulted in the formation of a doubly charged molecular fragment, the yield of which was measured as a function of the delay time between the pump and probe pulses. The measurements showed the presence of oscillations in the product yield with a period of less than 4.5 fs, which is much shorter than the characteristic times of the vibrational response of the system associated with the motion of nuclei. The results of the experiment were explained in terms of the ultrafast dynamics of the electron wave packet, which manifest itself in periodic variations in the charge density in the region of the amino group, which, apparently, affect the efficiency of absorption of the probing pulse energy by the amino group and thus provide the observed variations in the product yield.

The examples given above illustrate the promise of using attosecond pulses to study intramolecular electron dynamics. Information about the details of these dynamics is important for understanding chemical reactions and biological processes. The development of the attosecond experiment technique provided tools for inducing electronic processes, observing them in real time, and, eventually, controlling them. It appears to be possible to study even more complex intramolecular dynamics, in which both electrons and nuclei are involved. At the initial stage in such processes, as a rule, the response of electrons as much lighter particles dominates. As a result of photoionization of a molecule under the action of an attosecond pulse, coherent superpositions of electronic states of the parent molecular ion are created. Further, the ultrafast emission of an electron can also initiate nuclear dynamics, which in turn can lead to the breakdown of electronic coherence. Factors affecting the decoherence of electronic motion and the role of nuclear motion in such processes are important fundamental questions facing attosecond science, in particular, attosecond quantum control. According to recent calculations, the time of electron decoherence after photoionization of molecules can be only a few femtoseconds [229, 230]. The importance of such studies is dictated by the important role that electronic coherence plays in many chemical processes, among other things, presumably in ensuring the high efficiency of energy conversion during photosynthesis [231].

4.3 Attosecond control of electronic processes

Irradiation of targets with a combination of synchronized pulses of femtosecond IR and attosecond VUV or X-ray radiation with a variable delay between them opens up great opportunities not only for probing attosecond quantum dynamics using the pump–probe method but also for controlling electronic processes on the attosecond time scale. The problems to be addressed in this case can be conditionally divided into two groups in accordance with the role played by the low- and high-frequency components of the total field in relation to each other.

In the first case, attosecond VUV radiation plays the role of a control field that ensures the formation of time-localized electron wave packets that are subject to further action from a strong IR laser field. Due to the ultrashort duration compared

to the period of the IR field, attosecond pulses can provide fast single-photon excitation or detachment of electrons from atoms in precisely specified phases of the laser field that can be used to control such processes in strong laser fields as HHG or above-threshold ionization [232–234]. Such high-precision control over the moment of ionization of an atom by varying the delay between the VUV and IR fields was first experimentally carried out in [234], where the application of this approach to control the efficiency of energy exchange between an intense IR laser field and electrons in the process of above-threshold ionization was demonstrated (controlling attosecond radiation with photon energies somewhat higher than the ionization potential of the atom was used). Experiments were also carried out to control HHG by controlling the ionization stage with the help of seed attosecond pulses [235, 236], which demonstrated a significant (up to fivefold) increase in the harmonic yield compared to that when using only an IR field, and the generation of high-order harmonics was also achieved at laser intensities below the atomic ionization threshold [237].

The second regime of controlling the ionization processes involves the use of femtosecond IR radiation as a control field. The control of the ion yield (using attosecond radiation with photon energies lower than or close to the ionization potential) was demonstrated in [238]. In this regime, the possibility of implementing electromagnetically induced transparency for VUV radiation due to the destructive interference of the probability amplitudes of multiphoton ($\omega_{\mathrm{VUV}} + n\omega_{\mathrm{IR}}$) ionization through different channels was shown [239]. Experiments were also carried out in which control was demonstrated not only with respect to the absorption integrated over the spectrum of attosecond radiation but also with respect to the relative absorption coefficient for individual harmonics that make up attosecond pulses [183] that, in particular, can be used as a method for the absorption-enabled formation of ultrashort VUV pulses. Thus, the results mentioned above are the first demonstrations of the extension to the VUV range of those ideas of controlling the optical properties of media and the radiation propagating in them through coherent manipulation of atoms and molecules, which were previously widely developed for the visible and IR ranges.

In a number of studies, the probing and control of the electron dynamics during dissociative ionization of molecules in a two-component field, which is a combination of a femtosecond IR pulse and a train of attosecond VUV pulses with an adjustable delay between these components, have been carried out. The dependence of the yield, distribution over dissociation channels, and angular distributions of fragments on the delay between field pulses was demonstrated both for the simplest molecules (H_2, D_2) [240] and for more complex molecules exhibiting a multielectron response (O_2) [241]. In [242], even greater possibilities are shown for using this approach to implement attosecond coherent control of molecular dynamics; namely, based on the example of the D_2 molecule, the use of controlled quantum interference of various channels of the evolution of the electronic subsystem was demonstrated for switching between the population of various excited electronic states of a neutral molecule on an attosecond time scale; it was also shown that such a switching could be the first step in the femtosecond control of the further dynamics of ionization and dissociation of a molecular system. The results of these experiments indicate that the attosecond electronic response of molecular systems can be used to control chemical reactions, i.e., for the development of attochemistry.

5. Conclusion

Over the more than 20 years that have passed since the first publications on the generation of attosecond pulses and the measurement of their characteristics [15, 29], attosecond physics has grown into a large interdisciplinary area of research at the interface between laser, atomic, and molecular physics aimed at producing and measuring light pulses of subfemtosecond duration and their use for probing ultrafast processes caused by the dynamics of electrons in various media, as well as for controlling such processes. For further progress in this area of research, a number of serious problems need to be addressed, such as

(1) the development of high-power fiber and parametric laser sources of few-cycle light pulses (including those with a stabilized CE phase) for producing attosecond pulses (including isolated ones) with a high repetition rate (of the order of or more than 100 kHz);

(2) a significant increase in the intensity of attosecond pulses, up to the magnitudes required to implement the 'attosecond pump–attosecond probe' principle;

(3) attochirp compensation in a wide spectral region to obtain the shortest possible AP. In addition to the 'water window' covering the edges of the K-absorption bands of carbon, nitrogen, and oxygen, of great interest is the photon energy region of more than 500 eV, where the edges of the absorption bands of many practically important elements, including magnetic ones, are located;

(4) compensation of the electron magnetic drift as one of the main limiting factors [243] on the way to the generation of high harmonics with photon energies much higher than 1 keV using high-power mid-IR laser sources;

(5) producing intense attosecond pulses with high polarization ellipticity;

(6) developing techniques for measuring ultrashort light pulses, including in ordinary air, with a high repetition rate and in various frequency ranges;

(7) extension of the methods of attosecond spectroscopy developed using examples of atomic and simple molecular systems to the problems of studying the dynamics, including nonadiabatic, of more complex molecular systems, as well as condensed media.

Some ways to solve the above problems have been demonstrated in a number of recent papers [244–258].

In conclusion, it should be noted that, in recent years, along with sources based on HHG, sources such as free electron lasers (FELs) have been rapidly developing. Each of these two types of X-ray source has its own advantages. The brightness achieved by FELs in the X-ray range is many orders of magnitude higher than that of the sources based on HHG; at the same time, the latter provide an unprecedented high temporal resolution (of the order of 50 as) and the possibility of high-precision synchronization with external sources in the optical range, which formed the basis of many of the attosecond technologies described in the review. However, it should be noted that, in recent years, significant progress has been made in improving the temporal characteristics of FEL radiation. Among the various approaches to increasing the coherence of FEL radiation [259], the most significant is the use of coherent radiation provided by HHG as a seed for further amplification in FEL [260–262], which

creates the prerequisites for the creation of complex experimental stations exploiting the radiation of all these sources. Such stations can combine the use of narrow-band high-intensity FEL pulses, which induce photoionization of target particles from certain core shells, with an ultra-wideband attosecond supercontinuum covering the spectral range from the UV region to the water window and providing the implementation of multichannel attosecond absorption spectroscopy for probing the electronic and structural dynamics of the target near the edges of different absorption bands simultaneously [263].

This paper was supported by the Russian Foundation for Basic Research (grant no. 20-12-50293). V V Strelkov is grateful to the Theoretical Physics and Mathematics Advancement Foundation, Basis, for financial support.

References

1. Strelkov V V et al. *Phys. Usp.* **59** 425 (2016); *Usp. Fiz. Nauk* **186** 449 (2016)
2. Chang Z *Fundamentals of Attosecond Optics* (Boca Raton, FL: CRC Press, 2011)
3. Farkas Gy, Tóth Cs *Phys. Lett. A* **68** 447 (1992)
4. Antoine Ph, L'Huillier A, Lewenstein M *Phys. Rev. Lett.* **77** 1234 (1996)
5. Platonenko V T, Strelkov V V *Quantum Electron.* **27** 779 (1997); *Kvantovaya Electron.* **24** 799 (1997)
6. Korzhimanov A V et al. *Phys. Usp.* **54** 9 (2011); *Usp. Fiz. Nauk* **181** 9 (2011)
7. Wheeler J A et al. *Nat. Photon.* **6** 829 (2012)
8. Corkum P B *Phys. Rev. Lett.* **71** 1994 (1993)
9. Lewenstein M et al. *Phys. Rev. A* **49** 2117 (1994)
10. Kan C et al. *Phys. Rev. A* **52** R4336 (1995)
11. Gaarde M B et al. *Phys. Rev. A* **59** 1367 (1999)
12. Khokhlova M A, Strelkov V V *Phys. Rev. A* **93** 043416 (2016)
13. Salières P, L'Huillier A, Lewenstein M *Phys. Rev. Lett.* **74** 3776 (1995)
14. Balcou Ph et al. *Phys. Rev. A* **55** 3204 (1997)
15. Paul P M et al. *Science* **292** 1689 (2001)
16. Mairesse Y et al. *Science* **302** 1540 (2003)
17. Tzallas P et al. *Nature* **426** 267 (2003)
18. Agostini P, DiMauro L F *Rep. Prog. Phys.* **67** 813 (2004)
19. Scrinzi A et al. *J. Phys. B* **39** R1 (2006)
20. Frumker E et al. *Opt. Express* **20** 13878 (2012)
21. Quintard L et al. *Sci. Adv.* **5** eaau7175 (2019)
22. Veyrinas K et al. *Opt. Express* **29** 29813 (2021)
23. Platonenko V T, Strelkov V V *J. Opt. Soc. Am. B* **16** 435 (1999)
24. Platonenko V T, Strelkov V V, Ignatovich F V *Quantum Electron.* **29** 601 (1999); *Kvantovaya Electron.* **28** 43 (1999)
25. Bellini M et al. *Phys. Rev. Lett.* **81** 297 (1998)
26. López-Martens R et al. *Phys. Rev. Lett.* **94** 033001 (2005)
27. Kim K T et al. *Phys. Rev. A* **69** 051805 (2004)
28. Gustafsson E et al. *Opt. Lett.* **32** 1353 (2007)
29. Hentschel M et al. *Nature* **414** 509 (2001)
30. Goulielmakis E et al. *Science* **320** 1614 (2008)
31. Morlens A-S et al. *Opt. Lett.* **30** 1554 (2005)
32. Kim K T et al. *Phys. Rev. Lett.* **99** 223904 (2007)
33. Ko D H et al. *New J. Phys.* **12** 063008 (2010)
34. Zheng Y et al. *Phys. Rev. Lett.* **103** 043904 (2009)
35. Kohler M C, Keitel C H, Hatsagortsyan K Z *Opt. Express* **19** 4411 (2011)
36. Brabec Th, Krausz F *Rev. Mod. Phys.* **72** 545 (2000)
37. Paulus G G et al. *Nature* **414** 182 (2001)
38. Baltuška A et al. *Nature* **421** 611 (2003)
39. Liu X et al. *Phys. Rev. Lett.* **93** 263001 (2004)
40. Milošević D B et al. *J. Phys. B* **39** R203 (2006)
41. Kling M F et al. *Science* **312** 246 (2006)
42. Kreß M et al. *Nat. Phys.* **2** 327 (2006)
43. Silaev A A, Vvedenskii N V *Phys. Rev. Lett.* **102** 115005 (2009)
44. Nerush E N, Kostyukov I Yu *Phys. Rev. Lett.* **103** 035001 (2009)
45. Schiffrin A et al. *Nature* **493** 70 (2013)
46. Kübel M et al. *Phys. Rev. Lett.* **116** 193001 (2016)
47. Christov I P, Murnane M M, Kapteyn H C *Phys. Rev. Lett.* **78** 1251 (1997)
48. de Bohan A et al. *Phys. Rev. Lett.* **81** 1837 (1998)
49. Telle H R et al. *Appl. Phys. B* **69** 327 (1999)
50. Jones D J et al. *Science* **288** 635 (2000)
51. Apolonski A et al. *Phys. Rev. Lett.* **85** 740 (2000)
52. Baltuška A, Fuji T, Kobayashi T *Phys. Rev. Lett.* **88** 133901 (2002)
53. Kienberger R et al. *Nature* **427** 817 (2004)
54. Cavalieri A L et al. *New J. Phys.* **9** 242 (2007)
55. Wonisch A et al. *Appl. Opt.* **45** 4147 (2006)
56. Gaumnitz T et al. *Opt. Express* **25** 27506 (2017)
57. Strelkov V V et al. *Phys. Rev. A* **86** 013404 (2012)
58. Sola I J et al. *Nat. Phys.* **2** 319 (2006)
59. Corkum P B, Burnett N H, Ivanov M Y *Opt. Lett.* **19** 1870 (1994)
60. Strelkov V et al. *Appl. Phys. B* **78** 879 (2004)
61. Strelkov V et al. *J. Phys. B* **38** L161 (2005)
62. Platonenko V T, Strelkov V V *Quantum Electron.* **28** 749 (1998); *Kvantovaya Electron.* **25** 771 (1998)
63. Chang Z *Phys. Rev. A* **70** 043802 (2004)
64. Tcherbakoff O et al. *Phys. Rev. A* **68** 043804 (2003)
65. Sola I J et al. *Phys. Rev. A* **74** 013810 (2006)
66. Strelkov V et al. *Laser Phys.* **15** 871 (2005)
67. Sansone G et al. *Science* **314** 443 (2006)
68. Li J et al. *Nat. Commun.* **8** 186 (2017)
69. Tzallas P et al. *Nat. Phys.* **3** 846 (2007)
70. Skantzakis E et al. *Opt. Lett.* **34** 1732 (2009)
71. Feng X et al. *Phys. Rev. Lett.* **103** 183901 (2009)
72. Kim K T et al. *Phys. Rev. A* **69** 051805 (2004)
73. Strelkov V V et al. *J. Phys. B* **39** 577 (2006)
74. Pfeifer T et al. *Opt. Express* **15** 17120 (2007)
75. Hergott J-F et al. *Phys. Rev. A* **66** 021801 (2002)
76. Takahashi E, Nabekawa Y, Midorikawa K *Opt. Lett.* **27** 1920 (2002)
77. Nayak A et al. *Phys. Rev. A* **98** 023426 (2018)
78. Constant E et al. *Phys. Rev. Lett.* **82** 1668 (1999)
79. Kazamias S et al. *Phys. Rev. Lett.* **90** 193901 (2003)
80. Strelkov V V, Mével E, Constant E *New J. Phys.* **10** 083040 (2008)
81. Jullien A et al. *Appl. Phys. B* **93** 433 (2008)
82. Abel M J et al. *Chem. Phys.* **366** 9 (2009)
83. Calegari F et al., in *Multiphoton Processes and Attosecond Physics. Proc. of the 12th Intern. Conf. on Multiphoton Processes, ICOMP12 and the 3rd Intern. Conf. on Attosecond Physics, ATTO3* (Springer Proc. in Physics, Vol. 125, Eds K Yamanouchi, M Katsumi) (Heidelberg: Springer, 2012) p. 91
84. Gaarde M B, Schafer K J *Phys. Rev. Lett.* **89** 213901 (2002)
85. Gaarde M B, Schafer K J *Opt. Lett.* **31** 3188 (2006)
86. Roos L et al. *Phys. Rev. A* **60** 5010 (1999)
87. Toma E S et al. *J. Phys. B* **32** 5843 (1999)
88. Boutu W et al. *Phys. Rev. A* **84** 063406 (2011)
89. Dubrouil A et al. *Opt. Lett.* **36** 2486 (2011)
90. Treacher D J et al. *J. Opt.* **23** 015502 (2021)
91. Perry M D, Crane J K *Phys. Rev. A* **48** R4051 (1993)
92. Watanabe S et al. *Phys. Rev. Lett.* **73** 2692 (1994)
93. Mauritsson J et al. *Phys. Rev. Lett.* **97** 013001 (2006)
94. Pfeifer T et al. *Opt. Lett.* **31** 975 (2006)
95. Mashiko H et al. *Phys. Rev. Lett.* **100** 103906 (2008)
96. Zhao K et al. *Opt. Lett.* **37** 3891 (2012)
97. Bandulet H-C et al. *Phys. Rev. A* **81** 013803 (2010)
98. Kim I J et al. *Phys. Rev. Lett.* **94** 243901 (2005)
99. Geng J-W et al. *Phys. Rev. Lett.* **115** 193001 (2015)
100. Emelina A S et al. *Opt. Express* **24** 13971 (2016)
101. Vincenti H, Quéré F *Phys. Rev. Lett.* **108** 113904 (2012)
102. Akturk S et al. *J. Opt.* **12** 093001 (2010)
103. Vincenti H, Quéré F *Phys. Rev. Lett.* **108** 113904 (2012) see Supplemental Material, http://link.aps.org/supplemental/10.1103/PhysRevLett.108.113904
104. Kim K T et al. *Nat. Photon.* **7** 651 (2013)
105. Mashiko H, Suda A, Midorikawa K *Opt. Lett.* **29** 1927 (2004)
106. Major B et al. *Optica* **8** 960 (2021)
107. Bradley D J, Liddy B, Sleat W E *Opt. Commun.* **2** 391 (1971)
108. Schelev M Ya, Richardson M C, Alcock A J *Appl. Phys. Lett.* **18** 354 (1971)
109. Kane D J, Trebino R *Opt. Lett.* **18** 823 (1993)
110. Trebino R, Kane D J *J. Opt. Soc. Am. A* **10** 1101 (1993)
111. Iaconis C, Walmsley I A *Opt. Lett.* **23** 792 (1998)
112. Beck M et al. *Opt. Lett.* **18** 2041 (1993)
113. Walmsley I A, Wong V *J. Opt. Soc. Am. B* **13** 2453 (1996)
114. Constant E et al. *Phys. Rev. A* **56** 3870 (1997)
115. Isinger M et al. *Phil. Trans. R. Soc. A* **377** 20170475 (2019)
116. Véniard V, Taïeb R, Maquet A *Phys. Rev. A* **54** 721 (1996)
117. Varjú K et al. *J. Mod. Opt.* **52** 379 (2005)

118. Aseyev S A et al. *Phys. Rev. Lett.* **91** 223902 (2003)
119. Mairesse Y, Quéré F *Phys. Rev. A* **71** 011401 (2005)
120. Dinu L C et al. *Phys. Rev. Lett.* **91** 063901 (2003)
121. Kling M F, Vrakking M J J *Annu. Rev. Phys. Chem.* **59** 463 (2008)
122. Gallmann L, Cirelli C, Keller U *Annu. Rev. Phys. Chem.* **63** 447 (2012)
123. Haessler S et al. *New J. Phys.* **15** 013051 (2013)
124. Strelkov V *Phys. Rev. Lett.* **104** 123901 (2010)
125. Strelkov V V, Khokhlova M A, Shubin N Yu *Phys. Rev. A* **89** 053833 (2014)
126. Itatani J et al. *Phys. Rev. Lett.* **88** 173903 (2002)
127. Kitzler M et al. *Phys. Rev. Lett.* **88** 173904 (2002)
128. Drescher M et al. *Science* **291** 1923 (2001)
129. Smirnova O, Yakovlev V S, Ivanov M *Phys. Rev. Lett.* **94** 213001 (2005)
130. Yakovlev V S, Bammer F, Scrinzi A *J. Mod. Opt.* **52** 395 (2005)
131. Corkum P B, Krausz F *Nat. Phys.* **3** 381 (2007)
132. Krausz F, Ivanov M *Rev. Mod. Phys.* **81** 163 (2009)
133. Pfeifer T, Spielmann C, Gerber G *Rep. Prog. Phys.* **69** 443 (2006)
134. Orfanos I et al. *APL Photon.* **4** 080901 (2019)
135. Kosik E M et al. *J. Mod. Opt.* **52** 361 (2005)
136. Quéré F, Mairesse Y, Itatani J *J. Mod. Opt.* **52** 339 (2005)
137. Drescher M, Krausz F *J. Phys. B* **38** S727 (2005)
138. Schins J M et al. *J. Opt. Soc. Am. B* **13** 197 (1996)
139. Schins J M et al. *Phys. Rev. Lett.* **73** 2180 (1994)
140. Glover T E et al. *Phys. Rev. Lett.* **76** 2468 (1996)
141. Bouhal A et al. *J. Opt. Soc. Am. B* **14** 950 (1997)
142. Toma E S et al. *Phys. Rev. A* **62** 061801 (2000)
143. Ge Y *Phys. Rev. A* **74** 015803 (2006)
144. Goulielmakis E et al. *Science* **305** 1267 (2004)
145. Goulielmakis E et al. *Science* **317** 769 (2007)
146. Wirth A et al. *Science* **334** 195 (2011)
147. Krausz F, Stockman M I *Nat. Photon.* **8** 205 (2014)
148. Fattahi H et al. *Optica* **1** 45 (2014)
149. Kane D J *IEEE J. Quantum Electron.* **35** 421 (1999)
150. Gagnon J, Goulielmakis E, Yakovlev V S *Appl. Phys. B* **92** 25 (2008)
151. Lucchini M et al. *Opt. Express* **23** 29502 (2015)
152. Keathley P D et al. *New J. Phys.* **18** 073009 (2016)
153. Zhao X et al. *Phys. Rev. A* **95** 043407 (2017)
154. White J, Chang Z *Opt. Express* **27** 4799 (2019)
155. Kim K T et al. *New J. Phys.* **12** 083019 (2010)
156. Chini M et al. *Opt. Express* **18** 13006 (2010)
157. Walmsley I A, Dorrer C *Adv. Opt. Photon.* **1** 308 (2009)
158. Quéré F et al. *Phys. Rev. Lett.* **90** 073902 (2003)
159. Cormier E et al. *Phys. Rev. Lett.* **94** 033905 (2005)
160. Mairesse Y et al. *Phys. Rev. Lett.* **94** 173903 (2005)
161. Remetter T et al. *Nat. Phys.* **2** 323 (2006)
162. Dudovich N et al. *Nat. Phys.* **2** 781 (2006)
163. Kim K T et al. *Nat. Phys.* **9** 159 (2013)
164. Kim K T, Villeneuve D M, Corkum P B *Nat. Photon.* **8** 187 (2014)
165. Hoflund M et al. *Ultrafast Sci.* **2021** 9797453 (2021)
166. Kobayashi Y et al. *Opt. Lett.* **23** 64 (1998)
167. Nikolopoulos L et al. *Phys. Rev. Lett.* **94** 113905 (2005)
168. Nomura Y et al. *Nat. Phys.* **5** 124 (2009)
169. Sekikawa T et al. *Nature* **432** 605 (2004)
170. Tzallas P, Skantzakis E, Charalambidis D *J. Phys. B* **45** 074007 (2012)
171. Kosuge A et al. *Phys. Rev. Lett.* **97** 263901 (2006)
172. Nabekawa Y et al. *Phys. Rev. Lett.* **96** 083901 (2006)
173. Nabekawa Y et al. *Phys. Rev. Lett.* **97** 153904 (2006)
174. Shimizu T et al. *Phys. Rev. A* **75** 033817 (2007)
175. Takahashi E et al. *Nat. Commun.* **4** 2691 (2013)
176. Sekikawa T et al. *Opt. Express* **16** 21922 (2008)
177. Strelkov V V, Birulia V A, Magunov A I *New J. Phys.* **20** 093025 (2018)
178. Raz O et al. *Phys. Rev. Lett.* **107** 133902 (2011)
179. Raz O et al. *Opt. Express* **22** 24935 (2014)
180. Pedatzur O et al. *Nat. Photon.* **13** 91 (2019)
181. Muller H G *Appl. Phys. B* **74** s17 (2002)
182. Goulielmakis E et al. *Nature* **466** 739 (2010)
183. Holler M et al. *Phys. Rev. Lett.* **106** 123601 (2011)
184. Schultze M et al. *Science* **328** 1658 (2010)
185. Drescher M et al. *Nature* **419** 803 (2002)
186. Eisenbud L, PhD Thesis (Princeton, NJ: Princeton Univ., 1948)
187. Wigner E P *Phys. Rev.* **98** 145 (1955)
188. Smith F T *Phys. Rev.* **118** 349 (1960)
189. Dahlström J M, L'Huillier A, Maquet A *J. Phys. B* **45** 183001 (2012)
190. Ossiander M et al. *Nat. Phys.* **13** 280 (2016)
191. Cavalieri A L et al. *Nature* **449** 1029 (2007)
192. Neppl S et al. *Phys. Rev. Lett.* **109** 087401 (2012)
193. Mauritsson J et al. *Phys. Rev. Lett.* **105** 053001 (2010)
194. Klünder K et al. *Phys. Rev. Lett.* **106** 143002 (2011)
195. Swoboda M et al. *Phys. Rev. Lett.* **104** 103003 (2010)
196. Haessler S et al. *Phys. Rev. A* **80** 011404 (2009)
197. Caillat J et al. *Phys. Rev. Lett.* **106** 093002 (2011)
198. Huppert M et al. *Phys. Rev. Lett.* **117** 093001 (2016)
199. Gruson V et al. *Science* **354** 734 (2016)
200. Busto D et al. *J. Phys. B* **51** 044002 (2018)
201. Wang H et al. *Phys. Rev. Lett.* **105** 143002 (2010)
202. Wang X et al. *Appl. Opt.* **52** 323 (2013)
203. Beck A R, Neumark D M, Leone S R *Chem. Phys. Lett.* **624** 119 (2015)
204. Schultze M et al. *Nature* **493** 75 (2013)
205. Loh Z-H, Greene C H, Leone S R *Chem. Phys.* **350** 7 (2008)
206. Chini M et al. *Phys. Rev. Lett.* **109** 073601 (2012)
207. Beck A R et al. *New J. Phys.* **16** 113016 (2014)
208. Ott C et al. *Nature* **516** 374 (2014)
209. Bernhardt B et al. *Phys. Rev. A* **89** 023408 (2014)
210. Chen S et al. *Phys. Rev. A* **86** 063408 (2012)
211. Chini M et al. *Sci. Rep.* **3** 1105 (2013)
212. Muller H G, Tip A, van der Wiel M J *J. Phys. B* **16** L679 (1983)
213. Cheng Y et al. *Phys. Rev. A* **94** 023403 (2016)
214. Warrick E R et al. *J. Phys. Chem. A* **120** 3165 (2016)
215. Reduzzi M et al. *J. Phys. B* **49** 065102 (2016)
216. Liao C-T et al. *Phys. Rev. A* **95** 043427 (2017)
217. Ren X et al. *J. Opt.* **20** 023001 (2018)
218. Pertot Y et al. *Science* **355** 264 (2017)
219. Attar A R et al. *Science* **356** 54 (2017)
220. Chew A et al. *Phys. Rev. A* **97** 031407 (2018)
221. Saito N et al. *Optica* **6** 1542 (2019)
222. Kleine C et al. *J. Phys. Chem. Lett.* **10** 52 (2019)
223. Smith A D et al. *J. Phys. Chem. Lett.* **11** 1981 (2020)
224. Baggesen J C, Lindroth E, Madsen L B *Phys. Rev. A* **85** 013415 (2012)
225. Uiberacker M et al. *Nature* **446** 627 (2007)
226. Kelkensberg F et al. *Phys. Rev. Lett.* **103** 123005 (2009)
227. Sansone G et al. *Nature* **465** 763 (2010)
228. Calegari F et al. *Science* **346** 336 (2014)
229. Vacher M et al. *Phys. Rev. Lett.* **118** 083001 (2017)
230. Arnold C, Vendrell O, Santra R *Phys. Rev. A* **95** 033425 (2017)
231. Romero E et al. *Nat. Phys.* **10** 676 (2014)
232. Bandrauk A D, Shon N H *Phys. Rev. A* **66** 031401 (2002)
233. Schafer K J et al. *Phys. Rev. Lett.* **92** 023003 (2004)
234. Johnsson P et al. *Phys. Rev. Lett.* **95** 013001 (2005)
235. Biegert J et al. *Laser Phys.* **15** 899 (2005)
236. Heinrich A et al. *J. Phys. B* **39** S275 (2006)
237. Gademann G et al. *New J. Phys.* **13** 033002 (2011)
238. Johnsson P et al. *Phys. Rev. Lett.* **99** 233001 (2007)
239. Ranitovic P et al. *Phys. Rev. Lett.* **106** 193008 (2011)
240. Kelkensberg F et al. *Phys. Rev. Lett.* **107** 043002 (2011)
241. Siu W et al. *Phys. Rev. A* **84** 063412 (2011)
242. Ranitovic P et al. *Proc. Natl. Acad. Sci. USA* **111** 912 (2014)
243. Emelina A S, Emelin M Yu, Ryabikin M Yu *Quantum Electron.* **44** 470 (2014); *Kvantovaya Electron.* **44** 470 (2014)
244. Rothhardt J et al. *Opt. Express* **24** 18133 (2016)
245. Furch F J et al. *Opt. Lett.* **42** 2945 (2017)
246. Antonov V A et al. *Phys. Rev. Lett.* **123** 243903 (2019)
247. Fu Y et al. *Appl. Sci.* **8** 2451 (2018)
248. Chang Z *OSA Continuum* **2** 314 (2019)
249. Galloway B R et al. *Opt. Express* **24** 21818 (2016)
250. Zhai C et al. *Phys. Rev. A* **101** 053407 (2020)
251. Khokhlova M A et al. *Phys. Rev. A* **103** 043114 (2021)
252. Khairulin I R et al. *Sci. Rep.* **12** 6204 (2022)
253. Kubullek M et al. *Optica* **7** 35 (2020)
254. Korobenko A et al. *Optica* **7** 1372 (2020)
255. Neville S P et al. *Phys. Rev. Lett.* **120** 243001 (2018)
256. Timmers H et al. *Nat. Commun.* **10** 3133 (2019)
257. Zinchenko K S et al. *Science* **371** 489 (2021)
258. Rott F et al. *Struct. Dyn.* **8** 034104 (2021)
259. Pellegrini C, Marinelli A, Reiche S *Rev. Mod. Phys.* **88** 015006 (2016)
260. Lambert G et al. *Nat. Phys.* **4** 296 (2008)
261. Togashi T et al. *Opt. Express* **19** 317 (2011)
262. Ackermann S et al. *Phys. Rev. Lett.* **111** 114801 (2013)
263. Young L et al. *J. Phys. B* **51** 032003 (2018)